

# Investigation of *P. Vivax* Elimination via Mass Drug Administration

Md Nurul Anwar<sup>1\*</sup>, James M. McCaw<sup>1,2</sup>, Alexander E. Zarebski<sup>1</sup>, Roslyn I. Hickson<sup>1,3,4,†</sup>, and Jennifer A. Flegg<sup>1,†</sup>

<sup>1</sup>*School of Mathematics and Statistics, The University of Melbourne, Parkville, Australia*

<sup>2</sup>*Centre for Epidemiology and Biostatistics, Melbourne School of Population and Global Health, The University of Melbourne, Parkville, Australia*

<sup>3</sup>*Australian Institute of Tropical Health and Medicine, James Cook University, Townsville, Australia*

<sup>4</sup>*CSIRO, Townsville, Australia*

\* nurul.anwar@unimelb.edu.au † These authors contributed equally to this work

## Abstract

*Plasmodium vivax* is the most geographically widespread malaria parasite due to its ability to remain dormant (as a hypnozoite) in the human liver and subsequently reactivate. Given the majority of *P. vivax* infections are due to hypnozoite reactivation, targeting the hypnozoite reservoir with a radical cure is crucial for achieving *P. vivax* elimination. Stochastic effects can strongly influence dynamics when disease prevalence is low or when the population size is small. Hence, it is important to account for this when modelling malaria elimination. We use a stochastic multiscale model of *P. vivax* transmission to study the impacts of multiple rounds of mass drug administration (MDA) with a radical cure, accounting for superinfection and hypnozoite dynamics. Our results indicate multiple rounds of MDA with a high-efficacy drug are needed to achieve a substantial probability of elimination. This work has the potential to help guide *P. vivax* elimination strategies by quantifying elimination probabilities for an MDA approach.

**Keywords:** *P. vivax* elimination, stochastic model, hypnozoite, relapse, mass drug administration

## 1 Introduction

Among the five species of the *Plasmodium* parasite, *P. vivax* is the most geographically widespread and causes significant global morbidity and mortality [1, 2]. *P. vivax* has emerged as the dominant species in Southeast Asia and was responsible for 46% of cases (5.2 million total) in 2022 [3]. An

important characteristic of *P. vivax* is its ability to remain dormant in the human liver as a *hypnozoite*. *P. vivax* can remain dormant for up to a year, before reactivating and potentially causing onward transmission [4, 5]. Relapse events (where the hypnozoites reactivate) are responsible for more than 80% of *P. vivax* infections (in the absence of radical cure treatment) [6].

Despite the clinical significance of relapse, there is still uncertainty regarding the causes of hypnozoite reactivation. Some factors thought to be relevant include fever caused by other infections (such as *P. falciparum*), and recognition by the immune system of the same *Anopheles* specific protein (found in the salivary glands of adult female mosquitoes) [7, 8, 9].

It can be challenging to distinguish relapse from other types of recurrent malaria, such as reinfection or recrudescence. This can be due to incomplete elimination of a blood-stage infection, often associated with treatment failure [10]. Antimalarial drugs refer to those that clear either blood-stage or liver-stage parasites, with the specific recommended drugs depending on the parasite species.

Implementation of radical cure treatment is a part of standard case management in all *P. vivax* endemic settings. Targeting the hypnozoite reservoir is crucial in controlling or eliminating *P. vivax*, as transmission can be re-established from the reactivation of hypnozoites [9]. The 8-aminoquinoline class of drugs, such as primaquine and tafenoquine, clear hypnozoites from the liver, and are referred to as *radical cure* drugs [11, 12, 13]. The current treatment recommended by the WHO for *P. vivax* malaria is a combination of two antimalarial drugs: either chloroquine or artemisinin combination therapy (ACT) to clear parasites from the blood and either primaquine or tafenoquine to clear hypnozoites from the liver.

Mass drug administration (MDA) is a strategy used to control and eliminate malaria. MDA involves treating the entire at-risk population, or a well-defined sub-population, in a location with antimalarial drugs (depending on the malaria species), regardless of whether they have symptoms or a positive malaria diagnosis [14, 15]. In a radical cure MDA intervention (for *P. vivax*), individuals are typically given a combination of two drugs in line with the WHO-recommended treatment; one drug targets the blood-stage parasites and the other targets parasites in the liver. These radical cure MDA approaches aim to reduce both the blood-stage parasites and the size of the hypnozoite reservoir. However, there are costs to indiscriminant drug administration; primaquine and tafenoquine can cause life-threatening *haemolysis* in individuals with G6PD deficiency. G6PD deficiency is an enzymopathy affecting up to 30% of individuals in malaria-endemic regions [16]. Therefore, G6PD testing is recommended before administering 8-aminoquinoline.

Mathematical modelling has been widely used to understand the transmission of malaria, particularly *P. falciparum*, and the likely impact of interventions. *P. vivax* transmission differs from *P. falciparum* transmission, in that there are recurrent infections due to hypnozoite reactivation [9, 17, 18]. Mathematical models have been developed to study different aspects of *P. vivax* dynamics[19]: e.g. variation in hypnozoite numbers between infectious mosquito bites, the acquisition of immunity, superinfection (multiple simultaneous infections), and the effects of treatment. Many of the mathematical models use differential equations, as more analytical methods can be brought to bear on them, relative to stochastic or agent-based models.

When exploring disease elimination scenarios, stochastic effects can be important [20, 21]. Furthermore, when the population size is small, or the disease is at low prevalence, a stochastic model can provide more realistic representations of the transmission dynamics than deterministic models

[22, 23]. We have previously modelled hypnozoite acquisition, population dynamics and *P. vivax* transmission in a deterministic multiscale framework [17]. We also modelled the effect of the drug on both hypnozoite acquisition and infection, accounting for superinfection [18]. To the best of our knowledge, no other stochastic multiscale model has been developed that can consider *P. vivax* elimination while explicitly accounting for superinfection and the effects of multiple rounds of MDA on hypnozoite dynamics and *P. vivax* infection [19]. In this paper, we describe a stochastic multiscale model and demonstrate how this model can be used to compute the probability of *P. vivax* elimination under multiple MDA rounds.

## 2 Methods

### 2.1 Transmission model

We partition the human population based on individuals' *P. vivax* status. Let  $S$ ,  $I$ , and  $L$  represent the number of people in the human population who are *susceptible* to infection with no hypnozoites, *blood-stage infected* (with or without hypnozoites), and those who are *blood-stage negative but hypnozoite positive*, respectively.

While members within the  $I$  or  $L$  class may differ in the number of hypnozoites they have, we do not track this in our representation of the population. Instead, we model the distribution of the number of hypnozoites across the individuals in each class. This distribution is based on a stochastic, within-host model [24]. We assume a constant size for the human population, i.e.  $T_h = S + I + L$  is constant, where  $T_h$  is the human population size.

Let  $S_m$ ,  $E_m$  and  $I_m$  represent the number of mosquitoes that are susceptible, exposed, and infectious, where  $S_m, E_m, I_m \in \{0, 1, 2, \dots, T_m\}$  and  $S_m + E_m + I_m = T_m$ .  $T_m$  is not fixed and varies seasonally due to a varying birth rate,  $\theta(t)$ , given by

$$\theta(t) = g \left( 1 + \eta \cos \left( \frac{2\pi t}{365} \right) \right), \quad (1)$$

where  $g$  is the baseline mosquito birth (and death) rate and  $\eta \in [0, 1]$  is the seasonal amplitude. A schematic of the stochastic multiscale model is provided in Figure 1. Table 1 describes the possible compartment transitions and their associated rates, and Table 2 describes the value and source of the parameter values used.

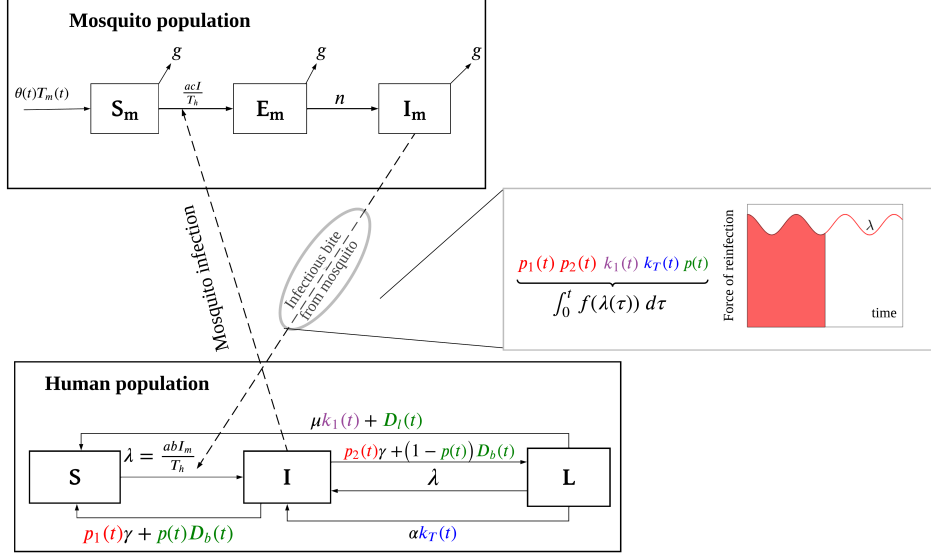


Figure 1: Schematic illustration of the multiscale model with treatment.  $S$ ,  $I$  and  $L$  represent the number of the human population that are susceptible with no hypnozoites, blood-stage infected (with or without hypnozoites), and blood-stage negative but hypnozoite positive, respectively. The left (top and bottom) part of the schematic demonstrates the transmission dynamics between the human and mosquito populations. The right part of the schematic demonstrates how the within-host model (see Supplementary Material) has been embedded within the population scale model. The within-host model takes into account the history of infective bites and calculates the probability of individuals in the  $I$  compartment having no hypnozoites and one blood-stage infection ( $p_1(t)$ ), individuals in the  $I$  compartment having at least one hypnozoite and one blood-stage infection ( $p_2(t)$ ), individuals in the  $L$  compartment having one hypnozoite ( $k_1(t)$ ), the expected size of the hypnozoite reservoir ( $k_T(t)$ ), and the probability of individuals in  $I$  having no hypnozoites ( $p(t)$ ) at any given time  $t$  as a function of the force of reinfection,  $\lambda(t)$ . We account for superinfection through the parameters  $p_1(t)$  and  $p_2(t)$ . The functions  $D_b(t)$  and  $D_l(t)$  capture the effect of treatment when implemented. Other parameters are defined in Table 2.

Table 1: Table of transition rates and stoichiometries for the stochastic multiscale model.

Event	Stoichiometries	Rate
Infection of individual in $S$ compartment	$(S, I, L, S_m, E_m, I_m) \rightarrow (S - 1, I + 1, L, S_m, E_m, I_m)$	$abSI_m/T_h$
Infection of individual in $L$ compartment	$(S, I, L, S_m, E_m, I_m) \rightarrow (S, I + 1, L - 1, S_m, E_m, I_m)$	$abLI_m/T_h$
Relapse of individual in $L$ compartment	$(S, I, L, S_m, E_m, I_m) \rightarrow (S, I + 1, L - 1, S_m, E_m, I_m)$	$\alpha k_T(t)L$
Death of last hypnozoite in individual in $L$ compartment	$(S, I, L, S_m, E_m, I_m) \rightarrow (S + 1, I, L - 1, S_m, E_m, I_m)$	$\mu k_1(t)L$
Natural recovery from $I$ compartment without hypnozoites	$(S, I, L, S_m, E_m, I_m) \rightarrow (S + 1, I - 1, L, S_m, E_m, I_m)$	$p_1(t)\gamma I$
Natural recovery from $I$ compartment (with hypnozoites)	$(S, I, L, S_m, E_m, I_m) \rightarrow (S, I - 1, L + 1, S_m, E_m, I_m)$	$p_2(t)\gamma I$
Recovery from $I$ compartment (without hypnozoites) due to radical cure	$(S, I, L, S_m, E_m, I_m) \rightarrow (S + 1, I - 1, L, S_m, E_m, I_m)$	$p(t)D_b(t)I$
Recovery from $I$ compartment (with hypnozoites) due to radical cure	$(S, I, L, S_m, E_m, I_m) \rightarrow (S, I - 1, L + 1, S_m, E_m, I_m)$	$(1 - p(t))D_b(t)I$
Recovery from $L$ compartment due to radical cure	$(S, I, L, S_m, E_m, I_m) \rightarrow (S + 1, I, L - 1, S_m, E_m, I_m)$	$D_l(t)L$
Birth of mosquitoes	$(S, I, L, S_m, E_m, I_m) \rightarrow (S, I, L, S_m + 1, E_m, I_m)$	$\theta(t)T_m(t)$
Mosquito exposure to sporozoite	$(S, I, L, S_m, E_m, I_m) \rightarrow (S, I, L, S_m - 1, E_m + 1, I_m)$	$acS_m I/T_h$
Mosquito becomes infectious	$(S, I, L, S_m, E_m, I_m) \rightarrow (S, I, L, S_m, E_m - 1, I_m + 1)$	$nE_m$
Death of susceptible mosquito	$(S, I, L, S_m, E_m, I_m) \rightarrow (S, I, L, S_m - 1, E_m, I_m)$	$gS_m$
Death of exposed mosquito	$(S, I, L, S_m, E_m, I_m) \rightarrow (S, I, L, S_m, E_m - 1, I_m)$	$gE_m$
Death of infectious mosquito	$(S, I, L, S_m, E_m, I_m) \rightarrow (S, I, L, S_m, E_m, I_m - 1)$	$gI_m$

Table 2: Definitions, values and sources for model parameters. The parameter ranges indicated in square brackets were used in the sensitivity analysis.

Symbol	Definition	Value/s	Source
$a$	Biting rate of mosquitoes	80 year <sup>-1</sup>	[25]
$b$	Transmission probability: mosquito to human	0.5	[26]
$c$	Transmission probability: human to mosquito	0.23	[27]
$\theta(t)$	Mosquito birth rate (seasonal)	Time-varying	Equation (1)
$g$	Baseline mosquito birth (and death) rate	0.1 day <sup>-1</sup>	[28]
$\eta$	Seasonal amplitude	0.1	Assumed
$T_h$	Population size of human	10,000	Assumed
$T_m(t)$	Population size of mosquito	Seasonal	Modelled
$T_m(0)$	Initial number of mosquito population	Calculated	$T_m(0) = m_0 T_h$
$m_0$	Initial mosquito to human ratio	Varied	
$n$	Rate of mosquito sporogony	1/12 days <sup>-1</sup>	[28]
$\gamma$	Recovery rate from $I$ compartment	1/60 day <sup>-1</sup>	[29]
$\alpha$	Hypnozoite activation rate	1/332 day <sup>-1</sup> [0, 1/100]	[9]
$\mu$	Hypnozoite death rate	1/425 day <sup>-1</sup> [0, 1/100]	[9]
$\nu$	Average number of hypnozoites per mosquito bite	8.5	[9]
$\lambda(t)$	Force of reinfection	Calculated	$\lambda(t) = abI_m/T_H$
$p(t)$	Probability that individual in $I$ has no hypnozoites within liver	Calculated	Equation (6)
$p_1(t)$	Probability that individual in $I$ has no hypnozoites and $MOI = 1$	Calculated	Equation (2)
$p_2(t)$	Probability that that individual in $I$ has hypnozoites and $MOI = 1$	Calculated	Equation (3)
$k_1(t)$	Probability that that individual in $L$ has 1 hypnozoite within liver	Calculated	Equation (S16)
$k_T(t)$	Average number of hypnozoites within liver for individual in $L$	Calculated	Equation (5)
$p_{\text{blood}}$	Probability that ongoing blood-stage infections are cleared instantaneously due to radical cure	0.9 [0.5, 1]	Assumed
$p_{\text{rad}}$	Probability that hypnozoites dies instantaneously due to radical cure	0.9 [0.5, 1]	[30]
$D_b(t)$	Clearance rate of blood-stage parasite due to radical cure	Calculated	Equation (7)
$D_l(t)$	Clearance rate of liver-stage parasite (hypnozoite) due to radical cure	Calculated	Equation (8)
$N_{\text{MDA}}$	Total number of MDA rounds	Varied	

Upon being bitten by an infected mosquito, humans in the  $S$  and  $L$  compartments transition to the blood-stage infected compartment ( $I$ ). The rate at which individuals from  $S$  and  $L$  transition to  $I$  is  $\lambda(t) = abI_m/T_h$ , where  $a$  is the mosquito biting rate and  $b$  is the probability of transmission from a mosquito bite.

To capture the hypnozoite dynamics and the variation of hypnozoites within individuals at the population level, we embed the within-host model of Mehra *et al.* [24] into our model to capture the additional structure within the  $I$  and  $L$  compartments. We use a mean-field approximation to obtain the probability distribution of hypnozoites within individuals. Here, we consider the short latency case, where hypnozoites can activate immediately following establishment. We assume the number of hypnozoites introduced by an infectious bite follows a geometric distribution with mean  $\nu$  and the dynamics of each hypnozoite are independent and identically distributed. Let  $H$ ,  $A$ ,  $C$ , and  $D$  represent states of establishment, activation, clearance (removal after activation) and death (removal before activation) of a hypnozoite, respectively. Each hypnozoite has two possible final states: death before activation ( $D$ ); or clearance after activation ( $C$ ). Furthermore, let  $N_f(t)$  denote the number of hypnozoites in states  $f \in F := \{H, A, C, D\}$  at time  $t$  and  $N_P(t)$ ,  $N_{PC}(t)$  denote the number of ongoing and cleared primary infections (an infection from an infectious mosquito bite), respectively, at time  $t$ . We then calculate the probability generating function (PGF) of  $N_f$ ,  $f \in F' := \{H, A, C, D, P, PC\}$  for the distribution of hypnozoites at time  $t$  for different states (see Supplementary Material for details).

Individuals in  $I$  transition to  $S$  at rate  $p_1(t)\gamma$ . Here,  $\gamma$  is the natural recovery rate from a blood-stage infection and  $p_1(t)$  is the probability that a blood-stage infected individual has no hypnozoites and only a single blood-stage infection (i.e. they do not have a superinfection). The derivation of  $p_1$  is given in the Supplementary Material and results in

$$p_1(t) = \frac{P(N_A(t) + N_P(t) = 1 | N_H(t) = 0) P(N_H(t) = 0)}{1 - P(N_A(t) + N_P(t) = 0)}, \quad (2)$$

where  $N_H(t)$ ,  $N_A(t)$ , and  $N_P(t)$  are the number of established hypnozoites in the liver, the number of relapses (that is, hypnozoites that have reactivated), and the number of primary infections, respectively. Individuals transition from  $I$  to  $L$  at the rate  $p_2(t)\gamma$ . Again,  $\gamma$  is the rate of natural recovery from a blood-stage infection, and now  $p_2(t)$  is the probability that a blood-stage infected individual has at least one hypnozoite and only one blood-stage infection (i.e. they do not have a superinfection.) As derived in the Supplementary Material, the equation for  $p_2$  is

$$p_2(t) = \frac{P(N_A(t) + N_P(t) = 1)}{1 - P(N_A(t) + N_P(t) = 0)} - p_1(t). \quad (3)$$

Furthermore, individuals transition from  $L$  to  $S$  at rate  $\mu k_1(t)$  where  $\mu$  is the hypnozoite death rate and  $k_1(t)$  is the probability that an individual in the  $L$  compartment has only a single hypnozoite:

$$k_1(t) = \frac{P(N_H(t) = 1 | N_A(t) = N_P(t) = 0)}{1 - P(N_H(t) = 0 | N_A(t) = N_P(t) = 0)}. \quad (4)$$

The rate individuals transition from  $L$  to  $I$  is  $\alpha k_T(t)$ , where  $\alpha$  is the hypnozoite activation rate and  $k_T(t)$  is the expected size of the hypnozoite reservoir within an individual in the  $L$  compartment.

The expected size of the hypnozoite reservoir is given by

$$k_T = \sum_{i=1}^{\infty} ik_i = \left( \frac{\mathbb{E}[N_H(t)|N_A(t) = N_P(t) = 0]}{1 - P(N_H(t) = 0|N_A(t) = N_P(t) = 0)} \right), \quad (5)$$

where  $\mathbb{E}[N_H(t)|N_A(t) = N_P(t) = 0]$  is the expected size of the hypnozoite reservoir in an uninfected (no blood-stage infection) individual.

## 2.2 Treatment

We assume drug treatment is administered at times  $t = s_1, s_2, \dots, s_{N_{\text{MDA}}}$ , where  $N_{\text{MDA}}$  is the total number of MDA rounds. Upon administration of the radical cure treatment, we assume the following: the blood-stage infections in an individual are instantaneously cleared with probability  $p_{\text{blood}}$ ; and each hypnozoite in the liver dies (independently) with probability  $p_{\text{rad}}$ . Therefore, whenever radical cure treatment is administered, individuals in the  $I$  compartment recover with probability  $p_{\text{blood}}$  and, depending on the hypnozoite reservoir, transition to compartment ( $S$ ) or compartment ( $L$ ). We define a probability  $p(t)$ , that a blood-stage infected individual has no hypnozoites in the liver immediately after the treatment:

$$\begin{aligned} p(t) &= P(N_H(t) = 0|N_A(t) > 0 \cup N_P(t) > 0) \\ &= \frac{P(N_H(t) = 0) - P(N_H(t) = N_A(t) = N_P(t) = 0)}{1 - P(N_A(t) = N_P(t) = 0)}. \end{aligned} \quad (6)$$

Assuming there is an MDA at time  $t$ , blood-stage infected individuals will transition to the susceptible compartment ( $S$ ) with probability  $p(t)D_b(t)$  and will transition to the  $L$  compartment with probability  $(1 - p(t))D_b(t)$ . Furthermore, individuals in the  $L$  compartment will transition to the compartment ( $S$ ) at an impulse  $D_l(t)$  due to the radical cure. The equations for  $D_b(t)$  and  $D_l(t)$  can be written as

$$D_b(t) = p_{\text{blood}} \sum_{j=1}^{N_{\text{MDA}}} \delta_D(t - s_j), \quad (7)$$

$$D_l(t) = \{k_1(t)p_{\text{rad}} + k_2(t)p_{\text{rad}}^2 + \dots\} \sum_{j=1}^{N_{\text{MDA}}} \delta_D(t - s_j), \quad (8)$$

where  $\delta_D(\cdot)$  is the Dirac delta function and  $s_j$ ,  $j = 1, 2, \dots, N_{\text{MDA}}$ , are the MDA administration times. That is, the functions  $D_b(t)$  and  $D_l(t)$  take effect only at the MDA administration time. As each hypnozoite will die with the probability  $p_{\text{rad}}$  due to the effect of radical cure drug, the liver-stage clearance impulse,  $D_l(t)$ , depends on how many hypnozoites are present in the liver. The time-dependent probabilities  $p(t)$ ,  $p_1(t)$ ,  $p_2(t)$ ,  $k_1(t)$ , and  $k_T(t)$  depend on the history of past infections (see Supplementary Material).

## 2.3 Objective of the study

Our primary objective here is to study the effect of a radical cure-based MDA intervention on the probability of *P. vivax* elimination. We construct an optimisation problem to obtain the optimal MDA timings reflecting that our objective is elimination. Since we use the mean-field approximation of the within-host model, here we optimise the deterministic version of the model



to avoid the added complexity. Though disease elimination may happen when prevalence is at a low level, for *P. vivax*, a low number of blood-stage infections may not be sufficient to guarantee elimination due to the re-established infection by the hypnozoite reservoir. Therefore, we define elimination to have occurred when there is no infection in the human and mosquito populations, i.e.,  $I + L + E_m + I_m = 0$ . Formally, the optimisation problem can be written as

$$\begin{aligned} & \underset{x_0, x_1, \dots, x_{N_{\text{MDA}}-1}}{\text{minimise}} && Z \\ & \text{s.t.} && x_1, x_2, \dots, x_{N_{\text{MDA}}-1} > 0, x_0 \geq 0 \text{ and } \sum x_i \leq t_{\text{max}}, \end{aligned}$$

where

$$Z = \int_{s_1}^{t_{\text{max}}} (I(t) + L(t) + E_m(t) + I_m(t)) dt$$

is the objective function and the  $x_i$ ,  $i = 1, 2, \dots, N_{\text{MDA}} - 1$  are the intervals between MDA rounds. That is, our objective is to minimise the area under the curve as keeping the total infection low for a longer duration (instead of at an instant) to encourage disease extinction. When seasonality is not considered, the time of the first MDA,  $s_1$ , can be considered arbitrary (as long as the dynamics have reached an equilibrium). However, when considering seasonality in the mosquito population, the time of the first MDA round is no longer arbitrary, as the dynamics display periodic oscillations around the mean annual prevalence of blood-stage infection. We defined  $x_0$  to be the interval between the first MDA round and the most recent peak prevalence. We minimise the objective function within a six-year period, starting from the first MDA round (e.g.,  $t_{\text{max}} = 6$  years).

Figure 2 summarises the optimal timing of each of the MDA rounds (up to 4 rounds) for varying initial mosquito to human ratios  $m_0$  (hence prevalence), under the model with seasonal dynamics. This figure is produced with the deterministic version of the stochastic model as in Anwar *et al.* [18] and shows that the optimal timing of the MDA does not vary considerably as a function of the initial mosquito to human ratio,  $m_0$ , especially when one (Figure 2A) and two (Figure 2B) MDA rounds are under consideration. However, there is variation in optimal MDA implementation times for three and four MDA rounds. For a higher initial mosquito ratio,  $m_0$ , the optimal interval between MDA rounds is longer (Figures 2C and D). Note that, with superinfection and seasonality in the mosquito population, a small number of initial mosquitoes can sustain a greater disease prevalence. We utilise these deterministic-model optimal timings in the stochastic model for up to four MDA rounds to study the impact of MDA with radical cure on *P. vivax* elimination. We also investigate another strategy referred to as ‘‘simplified MDA time’’, where we implement the first MDA round at a fixed time (after 5 years of burn-in). For this simplified approach the MDA rounds are implemented at 30-day intervals instead of the optimal. The optimal interval between the first and second rounds ( $x_1$ ) when up to four rounds are under consideration, stays close to 29 days when prevalence is 20-60% (see Table S1 and Figure S2 in Supplementary Material). Hence, we chose an interval of 30 days between all the rounds for the simplified approach. We compare the probability of elimination under this simplified strategy with the optimal strategies.

## 2.4 Model implementation

To efficiently simulate (approximate) trajectories from the stochastic model (see Algorithm 1) we use  $\tau$ -leaping [31]. Here, we use the mean-field approximation of the within-host model to obtain the time-dependent parameters  $p(t)$ ,  $p_1(t)$ ,  $p_2(t)$ ,  $k_1(t)$ , and  $k_T(t)$  which makes computation faster.

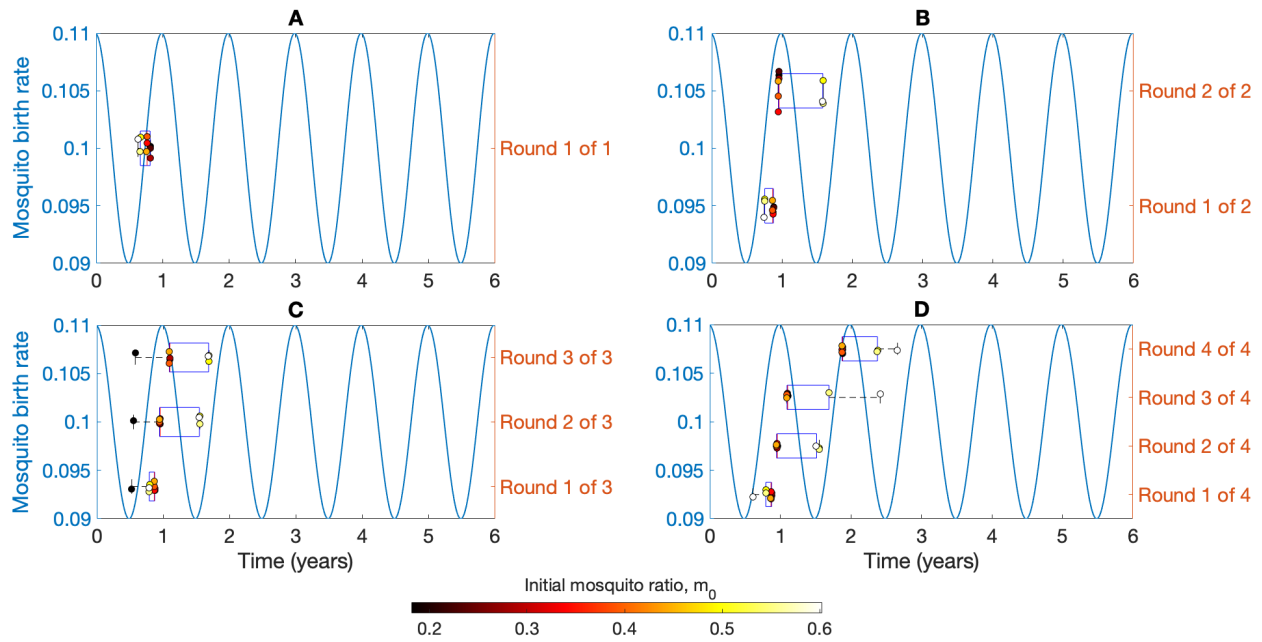


Figure 2: Optimal MDA times for up to four rounds (right vertical axis) obtained with the deterministic version of the model in reference to seasonal mosquito birth rate  $\theta(t)$  (left vertical axis). The box plot shows the distribution of the optimal MDA implementation times for different initial mosquito to human ratios to humans (coloured scattered points). These different initial mosquito ratios correspond to prevalence of blood-stage infection in the range 10–90%.

The initial conditions, including mosquito to human ratio were chosen to have a prevalence of blood-stage infection in the range of 10–90%, chosen to enable exploration of a wide range of prevalences. We used the MATLAB optimisation tool ‘Multistart’ with 50 different initial starting points in the range [1,365] and with *fmincon* (SQP algorithm) to generate global optimal solutions. All model parameters are described in Table 2. The optimisation model is implemented to start at year 5 to allow some burn-in period (we obtained the value of  $m_0$  using the deterministic model to obtain the equilibrium mean prevalence for the stochastic model).

---

**Algorithm 1:** Algorithm to approximate an exact trajectory of the stochastic model.

---

- 1 Define parameters. Choose  $\tau = 1$ . Initialise model with initial condition  $\{S(0), I(0), L(0), S_m(0), E_m(0), I_m(0)\}$ .
  - 2 **while**  $t < t_{end}$  *or*  $I + L + E_m + I_m = 0$ , **do**
  - 3     Calculate the time-dependent parameters  $p(t)$ ,  $p_1(t)$ ,  $p_2(t)$ ,  $k_1(t)$ , and  $k_T(t)$  using Equations (6), (2), (3), (S16), (5), respectively.
  - 4     Calculate all the event rates  $R_j$ ,  $j = 1, 2, \dots, 15$  as in Table 1.
  - 5     For each event  $E_j$ ,  $j = 1, 2, \dots, 12$  in Table 1, generate  $K_j \sim \text{Poisson}(R_j\tau)$  that provides the number of each event that occurs within the time interval  $[t, t + \tau]$ .
  - 6     Update the states  $\{S, I, L, S_m, E_m, I_m\}$  at time  $t + \tau$ .
- 

### 3 Results

We consider up to four rounds of MDA to study the impact of radical cure treatment on *P. vivax* elimination. Figure 3 presents the impact of one and four rounds of MDA on the number of humans in the *I* and *L* compartments. Here, the timings of the MDA rounds (vertical lines) are chosen to be the optimal MDA times from the deterministic model when the initial mosquito to human ratio is  $m_0 = 0.38$  ( $m_0$  is chosen here to have a moderate transmission intensity (70%)). Figures 3A and C depict the effect of one MDA round, while Figures 3B and D depict the effect of four MDA rounds on the number of humans in the *I* and *L* compartments, respectively. As we assume that the efficacy of the radical cure drug is 90%, the hypnozoite reservoir is never fully cleared when the drug is administered. Therefore, many individuals will transition to the *L* compartment, explaining the spikes in Figures 3C and D when the first round of MDA is administered. Under four MDA rounds, the median trajectories for both infections reach close to zero (Figures 3B, D) after the fourth round. However, new mosquito bites and hypnozoites from new bites, as well as those hypnozoites that survived the radical cure (because of imperfect drug efficacy), contribute to new infections. This drives the median trajectory for the number of blood-stage infections to eventually increase (Figures 3A, B), albeit with high levels of uncertainty.

*P. vivax* transmission dynamics are primarily dominated by hypnozoite dynamics as an estimated 79–96% of all *P. vivax* infections are due to relapse (in the absence of radical cure treatment) [32, 33, 34, 35, 36]. Hence, even if the number of blood-stage infections reaches zero, the activation of hypnozoites can contribute to new blood-stage infections, re-initiating or sustaining transmission. Figure 4 depicts the probability of elimination (green) and the probability of no blood-stage

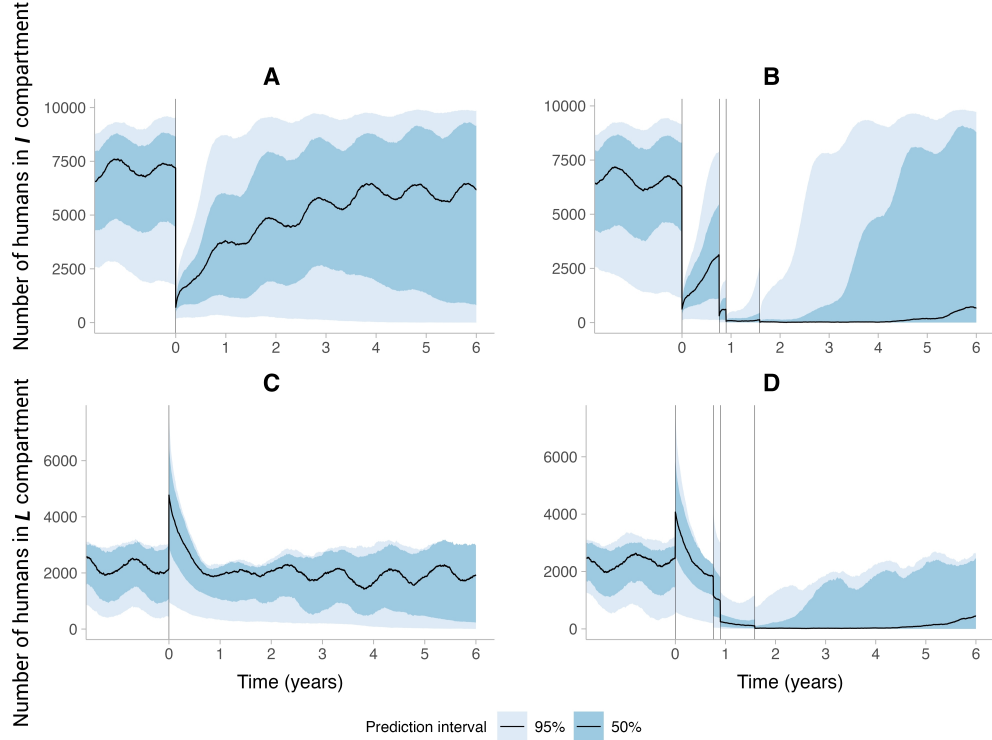


Figure 3: *Effect of one (first column) and four (second column) MDA rounds from 1000 simulations with  $T_h = 10000$ ,  $m_0 = 0.38$ . Subplots A and C illustrate the effect of one MDA round on the number of humans in the I and L compartments, respectively. Subplots B and D illustrate the effect of four MDA rounds, respectively. The median trajectory out of the 1000 trajectories is indicated by the black line with 50% and 95% prediction intervals shown in shading. The grey vertical lines indicate the time of each MDA round. Parameters are as in Table 2.*

infection (magenta) over time. Figures 4A and B depict the probability under one and four MDA rounds, respectively, when the initial mosquito to human ratio is  $m_0 = 0.38$ . The probability of elimination and the probability of no blood-stage infection under one MDA are very small (Figure 4A). That is, one MDA round does not have any epidemiologically relevant effect on the probability of elimination when the transmission intensity is moderate to high (for the assumed human population size,  $T_h = 10000$  and initial mosquito population size,  $T_m = 3800$ ). However, the probability of elimination and the probability of no blood-stage infection under four MDA rounds increases over time after the fourth MDA round and is epidemiological relevant (in terms of magnitude), see Figure 4B. Since we assume that any ongoing blood-stage infection will be cleared instantaneously due to the efficacy of the drug (here  $p_{\text{blood}} = 0.9$ ), the number of blood-stage infections is driven down to very low numbers immediately following the fourth MDA round (as per Figures 3B). The stochastic event of blood-stage elimination is more likely when blood-stage infection numbers are low, which explains why the probability of no blood-stage infection increases after the fourth MDA round. Furthermore, since we assume that hypnozoites in the liver are cleared instantaneously upon administration of the radical cure, the effect of radical cure on hypnozoites not only depends on the efficacy of the drug (here each hypnozoite is cleared with probability  $p_{\text{rad}} = 0.9$ ) but also on the hypnozoite reservoir size ( $k_T$ ). Activation of the hypnozoites that survive radical cure, and

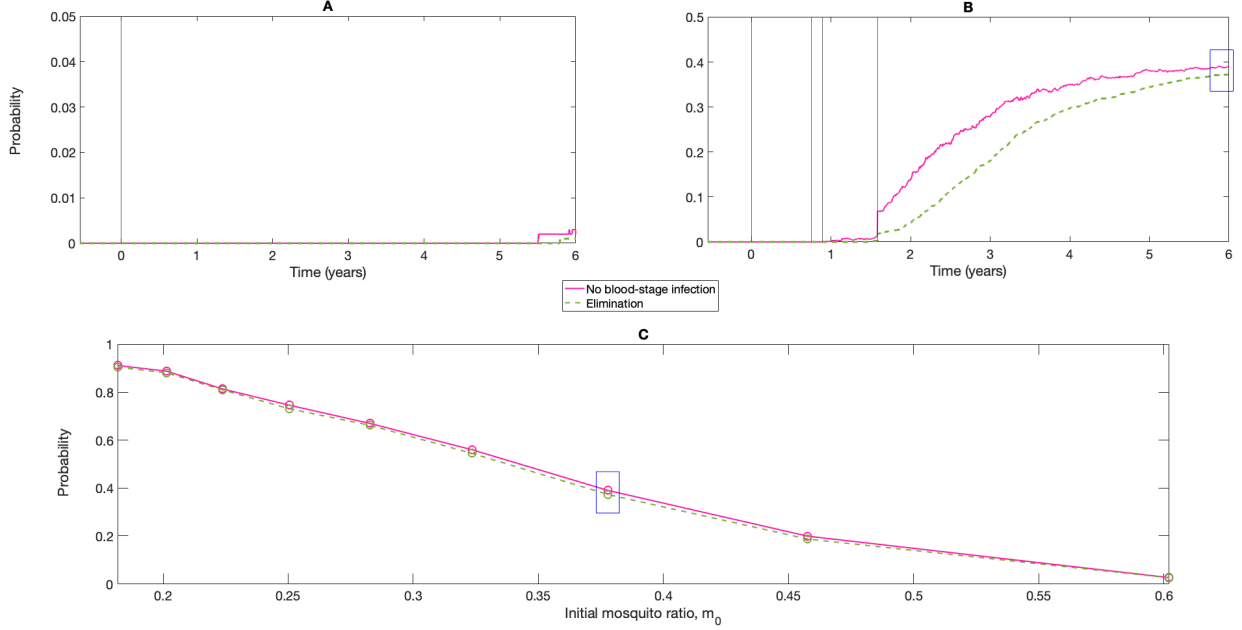


Figure 4: Probability of *P. vivax* elimination (green) and probability of no blood-stage infection (magenta) over time under one (Subplot A) and four (Subplot B) MDA rounds, respectively, with the initial mosquito to human ratio,  $m_0 = 0.38$ . The vertical lines indicate the MDA implementation times. Subplot C: Probability of *P. vivax* elimination and probability of no blood-stage infection for a varying number of initial mosquito to human ratios,  $m_0$ , under four MDA rounds. Probabilities are evaluated after six years from the first MDA round (from 1000 stochastic simulations). The blue box in Subplot C illustrates the evaluated probability in Subplot B. Note the different scales of the vertical axes in the subplots. Parameters are as in Table 2.

subsequent infectious mosquito bites, contribute to new blood-stage infections; thus the probability of no blood-stage infection over time is not monotonically increasing over time. This is distinct from the probability of elimination, which monotonically increases since elimination is an absorbing state of the system. The probability of elimination and the probability of no blood-stage infection vary across different transmission intensities. Figure 4C depicts the probability of elimination and the probability of no blood-stage infection under four rounds of MDA for varying initial mosquito to human ratios,  $m_0$ , six years after the first MDA round. The lower the initial mosquito to human ratio,  $m_0$ , the higher the probabilities of elimination and no blood-stage infection. We note that these results are for a fixed human population size,  $T_h = 10000$ ; the probability of elimination would vary with  $T_h$ .

The probabilities of *P. vivax* elimination after six years for up to four rounds of MDA, and no MDA, for varying initial mosquito to human ratios,  $m_0$ , are depicted in Figure 5. The overall impact of one MDA round (yellow line, Figure 5) is not substantially different compared to no MDA (red line, Figure 5), particularly as the initial mosquito ratio ( $m_0$ ) increases. When the initial mosquito to human ratio,  $m_0$ , is low, a small proportion of simulations fade out even if there are no rounds of MDA, which corresponds to a low probability of elimination. However, as the transmission in-

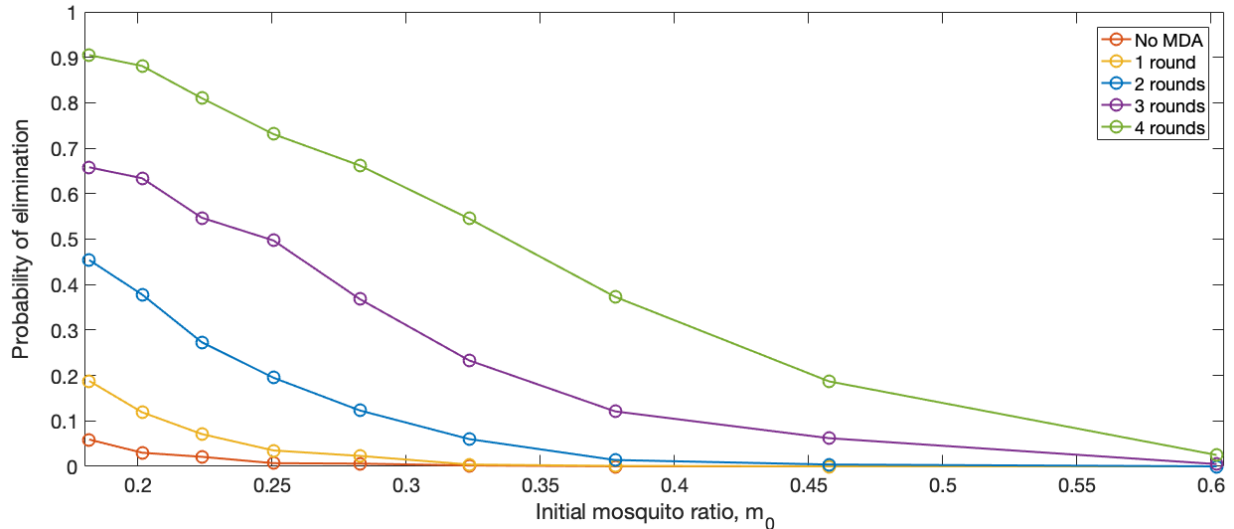


Figure 5: Effect of up to four rounds of MDA on the probability of *P. vivax* elimination after six years with varying number of initial mosquito to human ratios,  $m_0$ , compared to no MDA (red line) from 1000 stochastic simulations. Parameters are as in Table 2.

tensity increases with increasing  $m_0$ , there is negligible probability of elimination without MDA. As  $m_0$  increases, the probability of elimination decreases (regardless of MDA number and timing). Furthermore, the probability of elimination increases for fixed  $m_0$  as the number of MDA rounds increases. That is, with a higher number of MDA rounds (and  $m_0$  held fixed), the probability of *P. vivax* elimination is higher.

Hypnozoite dynamics and the efficacy of radical cure have a considerable influence on *P. vivax* transmission and elimination. Figure 6 illustrates the sensitivity of the probability of *P. vivax* elimination to some key model parameters under four rounds of MDA for a fixed  $m_0 = 0.38$ . The initial mosquito to human ratio  $m_0$  is chosen here to give a moderate transmission intensity and a moderate chance of *P. vivax* elimination after six years (see Figure 4C). Note that the timing of the four MDA rounds is derived optimally (using the deterministic version of the model) for the baseline set of parameter values (vertical line in each subplot in Figure 6) from Table 2. The residual variation evident in each subplot is due to the finite sample size (here 1000 model simulations were considered) used to compute Monte Carlo estimates for the probability of elimination. Figure 6A depicts the probability of elimination over the hypnozoite activation rate,  $\alpha$ , where the vertical line indicates the baseline rate as per Table 2. When the activation rate,  $\alpha$ , is zero, the only option for the hypnozoite is to die. In such cases, infectious mosquitoes are the only driver of ongoing disease transmission. Hence, with four rounds of MDA, there is a high chance of eliminating *P. vivax* with a probability very close to one. However, as we have assumed that radical cure does not provide protection from new infections, the disease may re-establish. As the activation rate,  $\alpha$ , increases from zero, relapse in addition to infectious bites contributes to onward transmission, and the probability of elimination decreases.

The probability of elimination as a function of the hypnozoite death rate,  $\mu$ , under four rounds of MDA is depicted in Figure 6B. If the hypnozoite death rate,  $\mu$ , is zero, the hypnozoites can only activate, increasing the disease burden, resulting in a very low probability of elimination (due

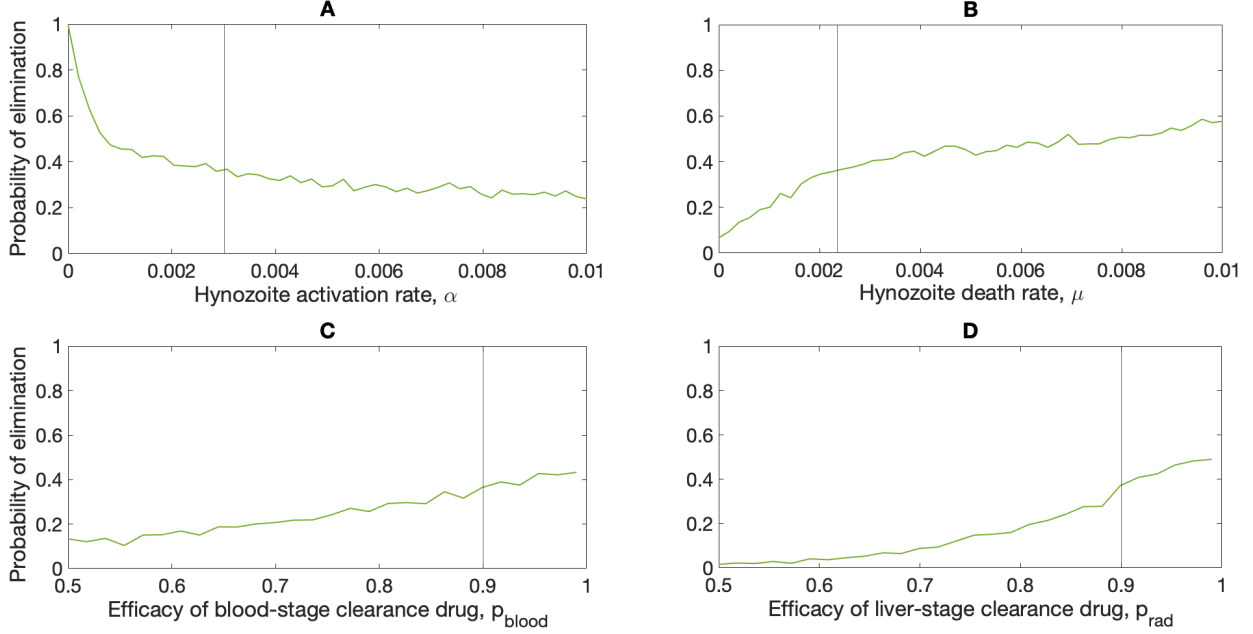


Figure 6: Sensitivity of probability of *P. vivax* elimination after six years over key model parameters under four rounds of MDA from 1000 stochastic simulations. Subplots A–D depict the probability of elimination over hypnozoite activation rate,  $\alpha$ , hypnozoite death rate,  $\mu$ , the efficacy of blood-stage clearance drug,  $p_{\text{blood}}$ , and the efficacy of liver-stage clearance drug,  $p_{\text{rad}}$ , respectively. The vertical line in each subplot indicates the baseline parameters used throughout Figures 2–5. Probabilities are evaluated after six years from the first MDA round. All other parameters are as in Table 2.

to stochasticity, some simulations still fade out). The probability of elimination increases as the hypnozoite death rate increases. That is, the higher the death rate,  $\mu$ , the higher the chance of elimination, as with hypnozoites dying more frequently, the disease burden from relapse decreases. Figures 6C–D depict the elimination probability for varying efficacy of the blood-stage and liver-stage drugs, respectively, when the other underlying parameters are as in Table 2. Unsurprisingly the probability of elimination increases with the efficacy of the blood-stage clearance drug and is the highest when 100% effective. The reason that the probability of elimination is not 100% when the blood-stage drug is 100% effective is that the effectiveness of the liver-stage clearance drug,  $p_{\text{rad}}$ , is set at the baseline value of 90%. Since it is possible that hypnozoites are not fully cleared, in addition to subsequent infectious mosquito bites, relapses can re-establish transmission. In the case of liver-stage drugs, the probability of elimination also increases with the efficacy of the liver-stage clearance drug,  $p_{\text{rad}}$ . Again, the more effective the drugs are, the higher the probability of elimination, peaking when 100% effective. It is worth noting that, radical cure with a low-efficacy drug, especially the liver-stage clearance drug, has little to no effect. That is, the chances of elimination improve with high-efficacy drugs.

We explored how much the specific timing for MDA implementation affects the probability of *P. vivax* elimination. To illustrate this, we use a simplified way of implementing four MDA rounds. Namely, we implement the MDA rounds with a 30-day interval instead of the optimal intervals (as determined using a deterministic analysis). We note that the choice of this 30-day interval is

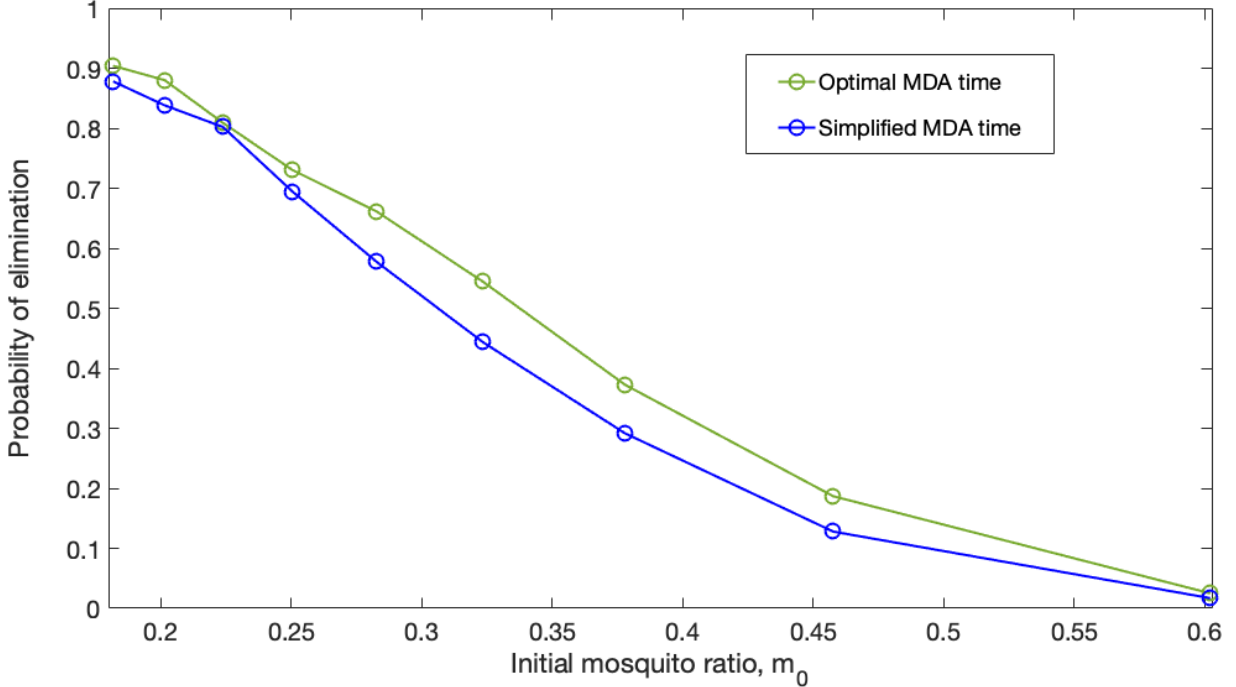


Figure 7: Probability of *P. vivax* elimination under four rounds of MDA with optimal timing (green line, timings of MDA decided as per the deterministic version of the model) compared to simplified MDA timing (blue solid line) for varying  $m_0$  with 1000 simulations. Probabilities are evaluated at year six from the first MDA round. All other parameters are as in Table 2.

influenced by the optimal intervals as discussed in Section 2.3. Figure 7 illustrates the probability of elimination under four MDA rounds with the optimal timing (green line) and compares to the simplified timing (blue line) for varying values of the initial mosquito to human ratio,  $m_0$ . Here, for every choice of the initial mosquito to human ratio,  $m_0$ , the optimal approach (as determined using the deterministic model) provides better results in terms of yielding a higher probability of elimination. However, the differences are not substantial and depending on other potential factors, policymakers could also consider a simplified strategy based on resources.

## 4 Discussion

As *P. vivax* transmission is primarily dominated by hypnozoite dynamics, targeting the hypnozoites with a radical cure to disrupt transmission is crucial to achieve the goal of *P. vivax* elimination [18, 37]. In this article, we study the impact of multiple rounds of MDA with radical cure on *P. vivax* elimination, defined to be when there are no infections in both human and mosquito populations. We previously studied the optimal interruption of *P. vivax* transmission with MDA under a deterministic multiscale model (see Anwar *et al.* [18]), but since this model was developed in a deterministic framework, disease elimination was not able to be considered. Here we have implemented a stochastic model to allow us to investigate elimination. We evaluate the probability of *P. vivax* elimination after six years from the first MDA, which has been chosen to fit with the current public health goals to achieve malaria elimination in at least 35 countries by 2030 according to WHO's Global Technical Strategy [38]. We observed that, as expected, the more MDA rounds



there are, the better the chance of *P. vivax* elimination (Figure 5). The administration times of the MDA rounds, when multiple MDA rounds are under consideration can affect the probability of elimination (Figure 7). Our results demonstrate that reductions in transmission due to MDA would likely be short-lived (unless elimination is achieved) as the underlying driver of transmission remains unchanged by the intervention. As the abundance of mosquitoes greatly affects *P. vivax* dynamics, the higher the mosquito population sizes are, the lower the probability of elimination, regardless of how many MDA rounds are considered, up to the four we explored (Figure 5). This is also true for the human population size (not explicitly shown here). We also observed that it is important to consider a radical cure with high efficacy (Figure 6D). Otherwise, the impact of MDA rounds on *P. vivax* elimination probability could be limited (this also depends on other model parameters). However, even with highly effective drugs and varying numbers of MDA rounds, elimination is anticipated to be unlikely with MDA alone (for example, the probability of elimination does not reach 100% for any parameter combinations considered in Figure 6).

The possibility of *P. vivax* elimination under MDA depends on many different factors, for example, how effective the drugs are and what proportion of the population is covered under MDA [39, 5]. In this work, we assumed that radical cure drugs are 90% effective in clearing both blood-stage parasites and hypnozoites, which falls in the estimated efficacy region of 57.7–95% (see Figures 6C–D) depending on the combination of drugs [40, 41, 42]. Since we explicitly model the impact of radical cure drugs on both blood-stage infections and hypnozoite dynamics, for simplicity, we assumed 100% treatment coverage in our model, which is difficult to achieve in reality due to various factors [43, 44]. Furthermore, human and mosquito movement in and out of the study area may also result in the potential reintroduction of infection, which we did not consider [45], though reactivation still results in a type of reintroduction into the target population. This means that, in regards to this parameter, our results are optimistic: our model’s estimate of the probability of elimination is an upper bound. Furthermore, because of the risk of hemolysis in G6PD-deficient individuals, radical cure is not recommended by the WHO without screening for G6PD deficiency [46, 47, 48]. Currently, We do not consider G6PD deficiency in our model. Therefore, accounting for G6PD deficiency is a potential avenue for future work and accounting for it will reduce the probability of elimination since fewer people will be able to take radical cure drugs.

Furthermore, because of the extensive use of antimalarial drugs, the parasite has developed resistance to some drugs, particularly chloroquine which is another reason MDA is not recommended. However, chloroquine is still effective in most parts of the world for *P. vivax* [49]. We currently do not consider drug resistance in our model. Moreover, the role of immunity can greatly influence how malaria dynamics progress through the population. However, we do not consider immunity. Individuals who have not previously experienced malaria infection almost invariably become infected when first exposed to infectious mosquito bites, as immunity against malaria has not yet developed [50]. Repeated exposure to infectious bites will still likely result in infection, though these individuals may be protected against severe malaria or death [50]. However, the immunity acquired from a primary infection may protect more strongly against relapses (which are genetically related to the primary infection) than against a new, genetically distinct primary infection [19]. This is because the parasites could be genetically identical or related, which could elicit a more protective immune response due to familiarity with the primary infection [51, 52]. Thus, relapses from the same batch of hypnozoites may be more likely only to cause asymptomatic infections. Since the multiscale model presented here depends on the history of past infections, including the role of immunity is, therefore, a potential future work as immunity against *P. vivax* strongly correlates to past infections.

From a methodological perspective, another limitation of our work is that we utilised the optimal MDA implementation times from a deterministic analysis of the stochastic version of the model. We also have not calibrated our model to any data. Therefore, all these are fruitful avenues for future work.

Mosquito dynamics greatly influence *P. vivax* dynamics, and as such, vector interventions, for example, long-lasting insecticide nets (LLIN) and indoor residual spray (IRS), should be considered along with MDA. Although we do not explicitly consider vector interventions in this paper, in areas where vector interventions are applied consistently, they can be implicitly considered through  $m_0$  by assuming an overall (constant) effect on the mosquito population (see Figure 7). We note there have been substantial efforts invested in explicitly exploring mosquito interventions [9, 53, 30]. The primary purpose of this work was to study the impact of MDA on *P. vivax* elimination; hence, studying the impact of MDAs along with other vector interventions is left for future work. Nonetheless, as our model accounts for stochasticity and hypnozoite dynamics with more detail than other published models, and we model the impact of MDA on each hypnozoite and infection independently, our research has the potential to contribute towards the goal of *P. vivax* elimination.

## Acknowledgement

This research was supported by The University of Melbourne’s Research Computing Services and the Petascale Campus Initiative. J.A. Flegg’s research is supported by the Australian Research Council (DP200100747, FT210100034) and the National Health and Medical Research Council (APP2019093). J.M. McCaw’s research is supported by the Australian Research Council (DP210101920) and the NHMRC Australian Centre of Research Excellence in Malaria Elimination (ACREME) (APP1134989). The contents of the published material are solely the responsibility of the individual authors and do not reflect the views of NHMRC.

## References

- [1] Spinello Antinori et al. “Biology of human malaria plasmodia including Plasmodium knowlesi”. In: *Mediterranean Journal of Hematology and Infectious Diseases* 4.1 (2012).
- [2] Katherine E Battle et al. “Mapping the global endemicity and clinical burden of Plasmodium vivax, 2000–17: a spatial and temporal modelling study”. In: *The Lancet* 394.10195 (2019), pp. 332–343.
- [3] WHO. *Consolidated Guidelines for malaria*. URL: <https://www.who.int/teams/global-malaria-programme/guidelines-for-malaria>(accessed:10.05.2023). (accessed: 10.05.2023).
- [4] Mallika Inwong et al. “Relapses of Plasmodium vivax infection usually result from activation of heterologous hypnozoites”. In: *The Journal of Infectious Diseases* 195.7 (2007), pp. 927–933.
- [5] Kamala Thriemer, Benedikt Ley, and Lorenz von Seidlein. “Towards the elimination of Plasmodium vivax malaria: Implementing the radical cure”. In: *PLoS Medicine* 18.4 (2021), e1003494.

- [6] Leanne J Robinson et al. “Strategies for understanding and reducing the Plasmodium vivax and Plasmodium ovale hypnozoite reservoir in Papua New Guinean children: a randomised placebo-controlled trial and mathematical model”. In: *PLoS Med* 12.10 (2015), e1001891.
- [7] Ivo Mueller et al. “Key gaps in the knowledge of Plasmodium vivax, a neglected human malaria parasite”. In: *The Lancet Infectious Diseases* 9.9 (2009), pp. 555–566.
- [8] Lena Hulden and Larry Hulden. “Activation of the hypnozoite: a part of Plasmodium vivax life cycle and survival”. In: *Malaria Journal* 10.1 (2011), p. 90.
- [9] Michael T White et al. “Modelling the contribution of the hypnozoite reservoir to Plasmodium vivax transmission”. In: *eLife* 3 (2014), e04692.
- [10] Mini Ghosh, Samson Olaniyi, and Olawale S Obabiyi. “Mathematical analysis of reinfection and relapse in malaria dynamics”. In: *Applied Mathematics and Computation* 373 (2020), p. 125044.
- [11] Timothy NC Wells, Jeremy N Burrows, and J Kevin Baird. “Targeting the hypnozoite reservoir of Plasmodium vivax: the hidden obstacle to malaria elimination”. In: *Trends in Parasitology* 26.3 (2010), pp. 145–151.
- [12] Walter RJ Taylor et al. “Short-course primaquine for the radical cure of Plasmodium vivax malaria: a multicentre, randomised, placebo-controlled non-inferiority trial”. In: *The Lancet* 394.10202 (2019), pp. 929–938.
- [13] Jeanne Rini Poespoprodjo et al. “Supervised versus unsupervised primaquine radical cure for the treatment of falciparum and vivax malaria in Papua, Indonesia: a cluster-randomised, controlled, open-label superiority trial”. In: *The Lancet Infectious Diseases* 22.3 (2022), pp. 367–376.
- [14] Gretchen Newby et al. “Review of mass drug administration for malaria and its operational challenges”. In: *The American Journal of Tropical Medicine and Hygiene* 93.1 (2015), p. 125.
- [15] Michelle S Hsiang et al. “Mass drug administration for the control and elimination of Plasmodium vivax malaria: an ecological study from Jiangsu province, China”. In: *Malaria Journal* 12.1 (2013), pp. 1–14.
- [16] Judith Recht, Elizabeth A Ashley, and Nicholas J White. “Use of primaquine and glucose-6-phosphate dehydrogenase deficiency testing: divergent policies and practices in malaria endemic countries”. In: *PLoS Neglected Tropical Diseases* 12.4 (2018), e0006230.
- [17] Md Nurul Anwar et al. “A Multiscale Mathematical Model of Plasmodium Vivax Transmission”. In: *Bulletin of Mathematical Biology* 84.8 (2022), pp. 1–24.
- [18] Md Nurul Anwar et al. “Optimal interruption of P. vivax malaria transmission using mass drug administration”. In: *Bulletin of Mathematical Biology* 85.6 (2023), p. 43.
- [19] Md Nurul Anwar et al. “A scoping review of mathematical models of Plasmodium vivax”. In: *arXiv preprint arXiv:2309.00274* (2023).
- [20] Klaus Henle, Stephen Sarre, and Kerstin Wiegand. “The role of density regulation in extinction processes and population viability analysis”. In: *Biodiversity & Conservation* 13.1 (2004), pp. 9–52.
- [21] Donald Ludwig. “Is it meaningful to estimate a probability of extinction?” In: *Ecology* 80.1 (1999), pp. 298–310.
- [22] Linda JS Allen and Amy M Burgin. “Comparison of deterministic and stochastic SIS and SIR models in discrete time”. In: *Mathematical Biosciences* 163.1 (2000), pp. 1–33.

- [23] Jan Beran. *Statistics for long-memory processes*. Vol. 61. CRC Press, 1994.
- [24] Somya Mehra et al. “Hypnozoite dynamics for *Plasmodium vivax* malaria: the epidemiological effects of radical cure”. In: *Journal of Theoretical Biology* (2022), p. 111014.
- [25] C Garrett-Jones. “The human blood index of malaria vectors in relation to epidemiological assessment”. In: *Bulletin of the World Health Organization* 30.2 (1964), p. 241.
- [26] David L Smith et al. “A quantitative analysis of transmission efficiency versus intensity for malaria”. In: *Nature Communications* 1.1 (2010), pp. 1–9.
- [27] Ajay R Bharti et al. “Experimental infection of the neotropical malaria vector *Anopheles darlingi* by human patient-derived *Plasmodium vivax* in the Peruvian Amazon”. In: *The American Journal of Tropical Medicine and Hygiene* 75.4 (2006), pp. 610–616.
- [28] Peter W Gething et al. “Modelling the global constraints of temperature on transmission of *Plasmodium falciparum* and *P. vivax*”. In: *Parasites & Vectors* 4.1 (2011), p. 92.
- [29] William E Collins, Geoffrey M Jeffery, and Jacquelin M Roberts. “A retrospective examination of anemia during infection of humans with *Plasmodium vivax*”. In: *The American Journal of Tropical Medicine and Hygiene* 68.4 (2003), pp. 410–412.
- [30] Narimane Nekkab et al. “Estimated impact of tafenoquine for *Plasmodium vivax* control and elimination in Brazil: A modelling study”. In: *PLoS Medicine* 18.4 (2021), e1003535.
- [31] Daniel T Gillespie. “Approximate accelerated stochastic simulation of chemically reacting systems”. In: *The Journal of Chemical Physics* 115.4 (2001), pp. 1716–1733.
- [32] Christine Luxemburger et al. “Treatment of vivax malaria on the western border of Thailand”. In: *Transactions of the Royal Society of Tropical Medicine and Hygiene* 93.4 (1999), pp. 433–438.
- [33] J Kevin Baird. *Real-world therapies and the problem of vivax malaria*. 2008.
- [34] Inoni Betuela et al. “Relapses contribute significantly to the risk of *Plasmodium vivax* infection and disease in Papua New Guinean children 1–5 years of age”. In: *The Journal of Infectious Diseases* 206.11 (2012), pp. 1771–1780.
- [35] Robert J Commons et al. “The effect of chloroquine dose and primaquine on *Plasmodium vivax* recurrence: a WorldWide Antimalarial Resistance Network systematic review and individual patient pooled meta-analysis”. In: *The Lancet Infectious Diseases* 18.9 (2018), pp. 1025–1034.
- [36] Robert J Commons et al. “Risk of *Plasmodium vivax* parasitaemia after *Plasmodium falciparum* infection: a systematic review and meta-analysis”. In: *The Lancet Infectious Diseases* 19.1 (2019), pp. 91–101.
- [37] Narimane Nekkab et al. “Accelerating towards *P. vivax* elimination with a novel serological test-and-treat strategy: a modelling case study in Brazil”. In: *The Lancet Regional Health–Americas* 22 (2023).
- [38] Joseph Mberikunashe et al. “Onyango P. Sangoro<sup>1</sup>, Ulrike Fillinger<sup>1</sup>, Kochelani Saili<sup>1, 2</sup>, Theresia Estomih Nkya<sup>1</sup>, Rose Marubu<sup>1</sup>, Freddie Masaninga<sup>3</sup>, Sonia Casimiro Trigo<sup>4</sup>, Casper Tarumbwa<sup>5</sup>, Busiku Hamainza<sup>6</sup>, Candrinho Baltazar<sup>7</sup>”. In: (2021).
- [39] Puji BS Asih, Din Syafruddin, and John Kevin Baird. “Challenges in the Control and Elimination of *Plasmodium vivax* Malaria”. In: *Towards Malaria Elimination: A Leap Forward* (2018), p. 77.

- [40] John H Huber et al. “How radical is radical cure? Site-specific biases in clinical trials underestimate the effect of radical cure on *Plasmodium vivax* hypnozoites”. In: *Malaria Journal* 20.1 (2021), pp. 1–15.
- [41] Erni J Nelwan et al. “Randomized trial of primaquine hypnozoitocidal efficacy when administered with artemisinin-combined blood schizontocides for radical cure of *Plasmodium vivax* in Indonesia”. In: *BMC Medicine* 13.1 (2015), pp. 1–12.
- [42] Alejandro Llanos-Cuentas et al. “Tafenoquine plus chloroquine for the treatment and relapse prevention of *Plasmodium vivax* malaria (DETECTIVE): a multicentre, double-blind, randomised, phase 2b dose-selection study”. In: *The Lancet* 383.9922 (2014), pp. 1049–1058.
- [43] Efundem Agboraw et al. “Factors influencing mass drug administration adherence and community drug distributor opportunity costs in Liberia: a mixed-methods approach”. In: *Parasites & Vectors* 14 (2021), pp. 1–11.
- [44] Timothy P Finn et al. “Treatment Coverage Estimation for Mass Drug Administration for Malaria with Dihydroartemisinin–Piperaquine in Southern Province, Zambia”. In: *The American Journal of Tropical Medicine and Hygiene* 103.2 Suppl (2020), p. 19.
- [45] Aatreyee M Das et al. “Modelling the impact of interventions on imported, introduced and indigenous malaria infections in Zanzibar, Tanzania”. In: *Nature communications* 14.1 (2023), p. 2750.
- [46] WHO. “Second focused review meeting of the Malaria Elimination Oversight Committee (MEOC): report of a virtual meeting, 28 June–1 July 2021”. In: (2021).
- [47] Rosalind E Howes et al. “G6PD deficiency prevalence and estimates of affected populations in malaria endemic countries: a geostatistical model-based map”. In: *PLoS Medicine* 9.11 (2012).
- [48] James Watson et al. “Implications of current therapeutic restrictions for primaquine and tafenoquine in the radical cure of vivax malaria”. In: *PLoS Neglected Tropical Diseases* 12.4 (2018), e0006440.
- [49] *Tackling antimalarial drug resistance*. <https://www.who.int/news/item/18-11-2022-tackling-emerging-antimalarial-drug-resistance-in-africa>. Accessed: 2023-05-10.
- [50] Jean Langhorne et al. “Immunity to malaria: more questions than answers”. In: *Nature Immunology* 9.7 (2008), pp. 725–732.
- [51] Nicholas J White. “Determinants of relapse periodicity in *Plasmodium vivax* malaria”. In: *Malaria Journal* 10.1 (2011), p. 297.
- [52] Chester J Joyner et al. “Humoral immunity prevents clinical malaria during *Plasmodium* relapses without eliminating gametocytes”. In: *PLoS Pathogens* 15.9 (2019), e1007974.
- [53] Michael T White et al. “Mathematical modelling of the impact of expanding levels of malaria control interventions on *Plasmodium vivax*”. In: *Nature Communications* 9.1 (2018), pp. 1–10.
- [54] Somya Mehra. “Epidemic models for malaria: superinfection”. MSc thesis. The University of Melbourne, 2022.
- [55] Ingemar Nasell. *Hybrid models of tropical infections*. Vol. 59. Springer Science & Business Media, 2013.

# Investigation of *P. Vivax* Elimination via Mass Drug Administration-Supplementary Material

Md Nurul Anwar<sup>1,\*</sup> James M. McCaw<sup>1,2</sup> Alexander E. Zarebski<sup>1</sup>, Roslyn I. Hickson<sup>1,3,4,†</sup> and Jennifer A. Flegg

<sup>1</sup>*School of Mathematics and Statistics, The University of Melbourne, Parkville, Australia*

<sup>2</sup>*Centre for Epidemiology and Biostatistics, Melbourne School of Population and Global Health, The University of Melbourne, Parkville, Australia*

<sup>3</sup>*Australian Institute of Tropical Health and Medicine, James Cook University, Townsville, Australia*

<sup>4</sup>*CSIRO, Townsville, Australia*

\*Corresponding author: nurul.anwar@unimelb.edu.au

†These authors contributed equally to this work

## S1 Within-host model

To capture the hypnozoite dynamics and its stochasticity within individuals, we embed a within-host model into our population level model. The within-host model was developed by Mehra *et al.* [24]. Our primary purpose in using the within-host model is to evaluate the probabilities  $p(t)$ ,  $p_1(t)$ ,  $p_2(t)$ ,  $k_1(t)$  and  $k_T(t)$  under multiple MDA rounds. These quantities describe aspects of the distribution of the hypnozoite reservoir and blood-stage infection within an individual; we use them to specify the dynamics at the population level.

Mosquito bites are modelled as a non-homogeneous Poisson process with rate  $\lambda(t)$ . Each bite introduces a batch of hypnozoites. The number of hypnozoites in the batch is geometrically distributed. The hypnozoites then independently progress through different states. This model can be considered as an infinite server queue process ( $M_t^X/G/\infty$ ) where  $X \sim \text{Geom}(\nu)$  [24].

Upon arrival within the host, hypnozoites enter a reservoir. Subsequently, each hypnozoite activates at a constant rate,  $\alpha$ , (which immediately triggers a blood-stage infection that is cleared at a constant rate,  $\gamma$ ) or dies at a constant rate,  $\mu$ , due to the death of the host cell. For the short-latency case (in which hypnozoites can immediately activate after establishment without going through a latency phase), a hypnozoite can be in one of four different states. Let  $H$ ,  $A$ ,  $C$ , and  $D$  represent states of establishment, activation, clearance (removal after activation) and death (removal before activation) of the hypnozoite, respectively. Each hypnozoite has two possible final states: death before activation ( $D$ ); or clearance after activation ( $C$ ). Figure S1 illustrates the possible trajectories of a single hypnozoite with and without any treatment.

The distribution of the state of a single hypnozoite (in the absence of treatment) is described by the following system of differential equations:

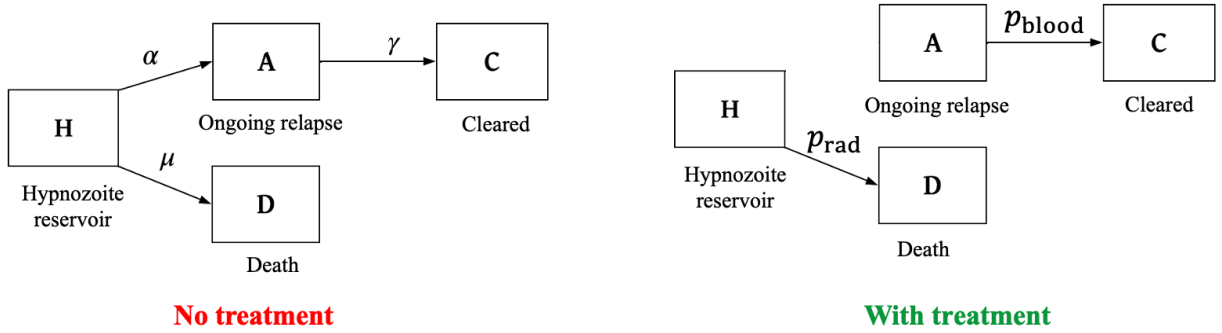


Figure S1: *The within-host model for a single hypnozoite without (left) and with treatment (right). The levels  $H$ ,  $A$ ,  $C$ , and  $D$  represent states of establishment, activation, clearance and death of the hypnozoite, respectively. Parameters  $p_{\text{blood}}$  and  $p_{\text{rad}}$  account for the instantaneous effect of the treatment.*

$$\begin{aligned}
 \frac{dp_H}{dt} &= -(\alpha + \mu)p_H, \\
 \frac{dp_A}{dt} &= \alpha p_H - \gamma p_A, \\
 \frac{dp_C}{dt} &= \gamma p_A, \\
 \frac{dp_D}{dt} &= \mu p_H,
 \end{aligned} \tag{S1}$$

with the initial condition  $\mathbf{p}(0) = (p_H(0), p_A(0), p_C(0), p_D(0)) = (1, 0, 0, 0)$ .

We can solve the equations to get the following distribution of the hypnozoite state through time:

$$\begin{aligned}
 p_H(t) &= e^{-(\alpha+\mu)t}, \\
 p_A(t) &= \frac{\alpha}{(\alpha + \mu) - \gamma} \left( e^{-\gamma t} - e^{-(\alpha+\mu)t} \right), \\
 p_C(t) &= \frac{\alpha}{\alpha + \mu} \left( 1 - e^{-(\alpha+\mu)t} \right) - \frac{\alpha}{(\alpha + \mu) - \gamma} \left( e^{-\gamma t} - e^{-(\alpha+\mu)t} \right), \\
 p_D(t) &= \frac{\mu}{\alpha + \mu} \left( 1 - e^{-(\alpha+\mu)t} \right).
 \end{aligned} \tag{S2}$$

### S1.1 Treatment model

Suppose that treatment is administered at times  $s_1 < s_2 < \dots < s_{N_{\text{MDA}}}$ . Considering a single hypnozoite, we denote its state at time  $t$  with  $X_r(t, s_1, s_2, \dots, s_{N_{\text{MDA}}}) \in \{H, A, C, D\}$  with corresponding PMF

$$p_H^r(t, s_1, \dots, s_{N_{\text{MDA}}}), p_A^r(t, s_1, \dots, s_{N_{\text{MDA}}}), p_C^r(t, s_1, \dots, s_{N_{\text{MDA}}}), p_D^r(t, s_1, \dots, s_{N_{\text{MDA}}}),$$

where the superscript “ $r$ ” is for radical cure. Note that, for  $t < s_1$ ,  $\mathbf{p}^r(t, s_1, s_2, s_3, \dots, s_{N_{\text{MDA}}}) = \mathbf{p}(t)$  as in Equation (S2). When the treatment is administered, any ongoing relapse will be cleared instantaneously with probability  $p_{\text{blood}}$  and each hypnozoite will die instantaneously with probability

$p_{\text{rad}}$ . The governing equations for the state probabilities under treatment (as described by Mehra *et al.* [24]) are

$$\frac{dp_H^r}{dt} = -(\alpha + \mu)p_H^r - \ln((1 - p_{\text{rad}}))^{-1} \sum_{j=1}^{N_{\text{MDA}}} \delta_D(t - s_j)p_H^r, \quad (\text{S3})$$

$$\frac{dp_A^r}{dt} = -\gamma p_A^r + \alpha p_H^r - \ln((1 - p_{\text{blood}}))^{-1} \sum_{j=1}^{N_{\text{MDA}}} \delta_D(t - s_j)p_A^r, \quad (\text{S4})$$

$$\frac{dp_C^r}{dt} = \gamma p_A^r + \ln((1 - p_{\text{blood}}))^{-1} \sum_{j=1}^{N_{\text{MDA}}} \delta_D(t - s_j)p_A^r, \quad (\text{S5})$$

$$\frac{dp_D^r}{dt} = -\mu p_H^r + \ln((1 - p_{\text{rad}}))^{-1} \sum_{j=1}^{N_{\text{MDA}}} \delta_D(t - s_j)p_H^r, \quad (\text{S6})$$

where  $\delta_D(\cdot)$  is the Dirac delta function. Due to the instantaneous assumption of the effect of treatment, the state probabilities  $\mathbf{p}^r(t, s_1, s_2, s_3, \dots, s_{N_{\text{MDA}}})$  will exhibit jump discontinuities at  $t = s_1, s_2, s_3, \dots, s_{N_{\text{MDA}}}$ .

The framework to account for continuous mosquito inoculation [24] assumes that

- the dynamics of hypnozoites are independent and identically distributed, with the PMF without treatment given by Equation (S2);
- infectious mosquito bites follow a non-homogeneous Poisson process with a time-dependent rate,  $\lambda(t)$ . The mean number of infectious bites in the interval  $(0, t]$  is  $q(t)$  where

$$q(t) = \int_0^t \lambda(\tau) d\tau; \quad (\text{S7})$$

- the number of hypnozoites established by each mosquito bite is geometrically-distributed ([9]) with mean  $\nu$ ;
- each infectious bite causes a primary infection which is cleared at rate  $\gamma$ ;
- and hypnozoites die due to the death of the host liver cell at rate  $\mu$  (e.g., there is no administration of anti-hypnozoital drugs).

Since we need the distribution of the size of the hypnozoite reservoir and infection status to use in our population-level model, we seek to obtain expressions for the quantities  $p(t)$ ,  $p_1(t)$ ,  $p_2(t)$ ,  $k_1(t)$  and  $k_T(t)$  from the within-host model under multiple rounds of MDA. Evaluating the quantities  $p(t)$ ,  $p_1(t)$ ,  $p_2(t)$ ,  $k_1(t)$  and  $k_T(t)$  in the population-level model requires the probability of hypnozoite establishment ( $p_H^r(t)$ ) and the probability of hypnozoite activation ( $p_A^r(t)$ ) [18]; hence we solve Equations (S3)–(S4) for  $N_{\text{MDA}}$  rounds for  $t \geq s_{N_{\text{MDA}}}$  to give

$$p_H^r(t, s_1, s_2, s_3, \dots, s_{N_{\text{MDA}}}) = (1 - p_{\text{rad}})^{N_{\text{MDA}}} p_H(t), \quad (\text{S8})$$

$$p_A^r(t, s_1, s_2, s_3, \dots, s_{N_{\text{MDA}}}) = (1 - p_{\text{blood}}) e^{-\gamma(t - s_{N_{\text{MDA}}})} p_A^r(s_{N_{\text{MDA}}}, s_1, s_2, \dots, s_{N_{\text{MDA}}-1}) + (1 - p_{\text{rad}})^{N_{\text{MDA}}} (p_A(t) - e^{-\gamma(t - s_{N_{\text{MDA}}})} p_A(s_{N_{\text{MDA}}})) , \quad (\text{S9})$$



where  $p_H(t)$  and  $p_A(t)$  are the probability of establishment and activation of a hypnozoite without treatment, respectively, and are given by Equation (??)

Let us define two additional states,  $P$  and  $PC$ , to denote an ongoing primary infection from infective mosquito bites and a cleared primary infection, respectively. Let  $N_f(t)$  denote the number of hypnozoites in states  $f \in F := \{H, A, C, D\}$  at time  $t$  and  $N_P(t)$ ,  $N_{PC}(t)$  denote the number of ongoing and cleared primary infections, respectively, at time  $t$ . For notational convenience, let  $F' := \{H, A, C, D, P, PC\}$ . We can now consider the random vector combining all of these variables:

$$\mathbf{N}(t) = (N_H(t), N_A(t), N_C(t), N_D(t), N_P(t), N_{PC}(t))$$

with  $\mathbf{N}(0) = \mathbf{0}$ . The PGF for  $\mathbf{N}$  can be written following from Equation (30) in Mehra *et al.* [24] (for short-latency case ( $k = 0$ ) with the probability of getting blood-stage infection after an infectious bite,  $p_{prim} = 1$ ) as

$$\begin{aligned} G(t, z_H, z_A, z_C, z_D, z_P, z_{PC}) &:= \mathbb{E} \left[ \prod_{f \in F'} z_f^{N_f(t)} \right], \\ &= \exp \left\{ -q(t) + \int_0^t \frac{\lambda(\tau) (z_P e^{-\gamma(t-\tau)} + (1 - e^{-\gamma(t-\tau)}) z_{PC})}{1 + \nu (1 - \sum_{f \in F} z_f p_f(t - \tau))} d\tau \right\}, \end{aligned} \quad (\text{S10})$$

where  $q(t)$  is the mean number of infective bites in the interval  $(0, t]$  and is given by Equation (S7).

The expression for the joint PGF with drug administration at time  $t = s_1$ , that is, under one round is given by Equation (31) in Mehra *et al.* [24]. Following a similar analysis, if the drug is administered at  $N_{\text{MDA}}$  successive times ( $t = s_1, s_2, \dots, s_{N_{\text{MDA}}}$ ), then the joint PGF for the number

of hypnozoites/infections in each state at time  $t$  is

$$\begin{aligned}
G^{s_1, s_2, \dots, s_{N_{\text{MDA}}}}(t, z_H, z_A, z_C, z_D, z_P, z_{PC}) &:= \mathbb{E} \left[ \prod_{f \in F'} z_f^{N_s^{s_1, s_2, \dots, s_{N_{\text{MDA}}}}(t)} \right], \\
= \begin{cases} \exp \left\{ -q(t) + \int_0^t \frac{\lambda(\tau)(z_P e^{-\gamma(t-\tau)} + (1-e^{-\gamma(t-\tau)})z_{PC})}{1+\nu(1-\sum_{f \in F} z_f p_f(t-\tau))} d\tau \right\} & \text{if } t < s_1 \\ \exp \left\{ -q(t) + \int_{s_1}^t \lambda(\tau) \frac{e^{-\gamma(t-\tau)} z_P + (1-e^{-\gamma(t-\tau)}) z_{PC}}{1+\nu(1-\sum_{f \in F} z_f p_f(t-\tau))} d\tau \right. \\ \quad \left. + \int_0^{s_1} \lambda(\tau) \frac{(1-p_{\text{blood}})e^{-\gamma(t-\tau)} z_P + (1-(1-p_{\text{blood}})e^{-\gamma(t-\tau)}) z_{PC}}{1+\nu(1-\sum_{f \in F} z_f p_s^r(t-\tau, s_1-\tau))} d\tau \right\} & \text{if } s_1 \leq t < s_2, \\ \exp \left\{ -q(t) + \int_{s_2}^t \lambda(\tau) \frac{e^{-\gamma(t-\tau)} z_P + (1-e^{-\gamma(t-\tau)}) z_{PC}}{1+\nu(1-\sum_{f \in F} z_f p_f(t-\tau))} d\tau \right. \\ \quad + \int_0^{s_1} \lambda(\tau) \frac{(1-p_{\text{blood}})e^{-\gamma(t-\tau)} z_P + (1-(1-p_{\text{blood}})e^{-\gamma(t-\tau)}) z_{PC}}{1+\nu(1-\sum_{f \in F} z_f p_s^r(t-\tau, s_1-\tau))} d\tau \\ \quad \left. + \int_{s_1}^{s_2} \lambda(\tau) \frac{(1-p_{\text{blood}})^2 e^{-\gamma(t-\tau)} z_P + (1-(1-p_{\text{blood}})^2 e^{-\gamma(t-\tau)}) z_{PC}}{1+\nu(1-\sum_{f \in F} z_f p_s^r(t-\tau, s_1-\tau, s_2-\tau))} d\tau \right\} & \text{if } s_2 \leq t < s_3, \\ \vdots \\ \exp \left\{ -q(t) + \int_{s_{N_{\text{MDA}}}}^t \lambda(\tau) \frac{e^{-\gamma(t-\tau)} z_P + (1-e^{-\gamma(t-\tau)}) z_{PC}}{1+\nu(1-\sum_{f \in F} z_f p_f(t-\tau))} d\tau \right. \\ \quad + \int_0^{s_1} \lambda(\tau) \frac{(1-p_{\text{blood}})e^{-\gamma(t-\tau)} z_P + (1-(1-p_{\text{blood}})e^{-\gamma(t-\tau)}) z_{PC}}{1+\nu(1-\sum_{f \in F} z_f p_s^r(t-\tau, s_1-\tau))} d\tau \\ \quad + \int_{s_1}^{s_2} \lambda(\tau) \frac{(1-p_{\text{blood}})^2 e^{-\gamma(t-\tau)} z_P + (1-(1-p_{\text{blood}})^2 e^{-\gamma(t-\tau)}) z_{PC}}{1+\nu(1-\sum_{f \in F} z_f p_s^r(t-\tau, s_1-\tau, s_2-\tau))} d\tau \\ \quad + \int_{s_2}^{s_3} \lambda(\tau) \frac{(1-p_{\text{blood}})^3 e^{-\gamma(t-\tau)} z_P + (1-(1-p_{\text{blood}})^3 e^{-\gamma(t-\tau)}) z_{PC}}{1+\nu(1-\sum_{f \in F} z_f p_s^r(t-\tau, s_1-\tau, s_2-\tau, s_3-\tau))} d\tau \\ \quad + \dots + \int_{s_{N-1}}^{s_{N_{\text{MDA}}}} \lambda(\tau) \frac{(1-p_{\text{blood}})^{N_{\text{MDA}}} e^{-\gamma(t-\tau)} z_P}{1+\nu(1-\sum_{f \in F} z_f p_s^r(t-\tau, s_1-\tau, s_2-\tau, s_3-\tau, \dots, s_{N_{\text{MDA}}}-\tau))} + \\ \quad \left. \frac{(1-(1-p_{\text{blood}})^{N_{\text{MDA}}} e^{-\gamma(t-\tau)}) z_{PC}}{1+\nu(1-\sum_{f \in F} z_f p_s^r(t-\tau, s_1-\tau, s_2-\tau, s_3-\tau, \dots, s_{N_{\text{MDA}}}-\tau))} d\tau \right\} & \text{if } t > s_{N_{\text{MDA}}}. \end{cases} \tag{S11}
\end{aligned}$$

We now use the PGF in Equations (S10) and (S11) to derive expressions for the probabilities  $p(t)$ ,  $k_1(t)$ ,  $k_T(t)$ ,  $p_1(t)$ , and  $p_2(t)$  under multiple MDA rounds.

## S1.2 Probability blood-stage infected individual has no hypnozoites: $p(t)$

We define  $p(t)$  as the probability that an individual has an empty hypnozoite reservoir conditional on an ongoing blood-stage infection (i.e. primary infection or relapse). That is,

$$\begin{aligned}
p(t) &= P(N_H(t) = 0 | N_A(t) > 0 \cup N_P(t) > 0) \\
&= \frac{P(N_H(t) = 0) - P(N_H(t) = N_A(t) = N_P(t) = 0)}{1 - P(N_A(t) = N_P(t) = 0)}, \tag{S12}
\end{aligned}$$

where the probability that an individual has an empty hypnozoite reservoir at time  $t$ ,  $P(N_H(t) = 0)$ , is given by

$$\begin{aligned}
P(N_H(t) = 0) &= G^{t, s_1, s_2, \dots, s_{N_{\text{MDA}}}}(t, z_H = 0, z_A = 1, z_C = 1, z_D = 1, z_P = 1, z_{PC} = 1), \\
&= \begin{cases} \exp\left\{-q(t) + \int_0^t \frac{\lambda(\tau)}{1+\nu p_H(t-\tau)} d\tau\right\} & \text{if } t < s_1, \\ \exp\left\{-q(t) + \int_{s_1}^t \frac{\lambda(\tau)}{1+\nu p_H(t-\tau)} d\tau + \int_0^{s_1} \frac{\lambda(\tau)}{1+\nu p_H^r(t-\tau, s_1-\tau)} d\tau\right. \\ \quad \left. + \int_{s_1}^{s_2} \frac{\lambda(\tau)}{1+\nu p_H^r(t-\tau, s_1-\tau, s_2-\tau)} d\tau\right\} & \text{if } s_1 \leq t < s_2, \\ \vdots & \\ \exp\left\{-q(t) + \int_{s_{N_{\text{MDA}}}}^t \frac{\lambda(\tau)}{1+\nu p_H(t-\tau)} d\tau + \int_0^{s_1} \frac{\lambda(\tau)}{1+\nu p_H^r(t-\tau, s_1-\tau)} d\tau\right. \\ \quad + \int_{s_1}^{s_2} \frac{\lambda(\tau)}{1+\nu p_H^r(t-\tau, s_1-\tau, s_2-\tau)} d\tau \\ \quad \left. + \dots + \int_{s_{N-1}}^{s_{N_{\text{MDA}}}} \frac{\lambda(\tau)}{1+\nu p_H^r(t-\tau, s_1-\tau, \dots, s_{N_{\text{MDA}}}-\tau)} d\tau\right\} & \text{if } t \geq s_{N_{\text{MDA}}}, \end{cases} \tag{S13}
\end{aligned}$$

the probability that an individual is neither experiencing a relapse nor a primary infection at time  $t$ ,  $P(N_A(t) + N_P(t) = 0)$  (i.e., no blood-stage infection), is given by

$$\begin{aligned}
P(N_A(t) + N_P(t) = 0) &= G^{t, s_1, s_2, \dots, s_{N_{\text{MDA}}}}(t, z_H = 1, z_A = 0, z_C = 1, z_D = 1, z_P = 0, z_{PC} = 1), \\
&= \begin{cases} \exp\left\{-q(t) + \int_0^t \frac{\lambda(\tau)(1-e^{-\gamma(t-\tau)})}{1+\nu p_A(t-\tau)} d\tau\right\} & \text{if } t < s_1, \\ \exp\left\{-q(t) + \int_{s_1}^t \frac{\lambda(\tau)(1-e^{-\gamma(t-\tau)})}{1+\nu p_A(t-\tau)} d\tau + \int_0^{s_1} \frac{\lambda(\tau)(1-(1-p_{\text{blood}})e^{-\gamma(t-\tau)})}{1+\nu p_A^r(t-\tau, s_1-\tau)} d\tau\right. \\ \quad \left. + \int_{s_1}^{s_2} \frac{\lambda(\tau)(1-(1-p_{\text{blood}})^2 e^{-\gamma(t-\tau)})}{1+\nu p_A^r(t-\tau, s_1-\tau, s_2-\tau)} d\tau\right\} & \text{if } s_1 \leq t < s_2, \\ \vdots & \\ \exp\left\{-q(t) + \int_{s_{N_{\text{MDA}}}}^t \frac{\lambda(\tau)(1-e^{-\gamma(t-\tau)})}{1+\nu p_A(t-\tau)} d\tau\right. \\ \quad + \int_0^{s_1} \frac{\lambda(\tau)(1-(1-p_{\text{blood}})e^{-\gamma(t-\tau)})}{1+\nu p_A^r(t-\tau, s_1-\tau)} d\tau \\ \quad + \int_{s_1}^{s_2} \frac{\lambda(\tau)(1-(1-p_{\text{blood}})^2 e^{-\gamma(t-\tau)})}{1+\nu p_A^r(t-\tau, s_1-\tau, s_2-\tau)} d\tau \\ \quad \left. + \dots + \int_{s_{N-1}}^{s_{N_{\text{MDA}}}} \frac{\lambda(\tau)(1-(1-p_{\text{blood}})^{N_{\text{MDA}}} e^{-\gamma(t-\tau)})}{1+\nu p_A^r(t-\tau, s_1-\tau, \dots, s_{N_{\text{MDA}}}-\tau)} d\tau\right\} & \text{if } t \geq s_{N_{\text{MDA}}}, \end{cases} \tag{S14}
\end{aligned}$$

and the probability that an individual is neither experiencing an infection nor has any hypnozoites

in their liver at time  $t$ ,  $P(N_H(t) = N_A(t) = N_P(t) = 0)$ , is given by

$$\begin{aligned}
& P(N_H(t) = N_A(t) = N_P(t) = 0) \\
& = G^{t, s_1, s_2, \dots, s_{N_{\text{MDA}}}}(t, z_H = 0, z_A = 0, z_C = 1, z_D = 1, z_P = 0, z_{PC} = 1), \\
& = \begin{cases} \exp\left\{-q(t) + \int_0^t \frac{\lambda(\tau)(1-e^{-\gamma(t-\tau)})}{1+\nu(p_H(t-\tau)+p_A(t-\tau))} d\tau\right\} & \text{if } t < s_1, \\ \exp\left\{-q(t) + \int_{s_1}^t \frac{\lambda(\tau)(1-e^{-\gamma(t-\tau)})}{1+\nu(p_H(t-\tau)+p_A(t-\tau))} d\tau\right. \\ \quad \left. + \int_0^{s_1} \frac{\lambda(\tau)(1-(1-p_{\text{blood}})e^{-\gamma(t-\tau)})}{1+\nu(p_H^r(t-\tau, s_1-\tau)+p_A^r(t-\tau, s_1-\tau))} d\tau\right\} & \text{if } s_1 \leq t < s_2, \\ \vdots \\ \exp\left\{-q(t) + \int_{s_{N_{\text{MDA}}}}^t \frac{\lambda(\tau)(1-e^{-\gamma(t-\tau)})}{1+\nu(p_H(t-\tau)+p_A(t-\tau))} d\tau\right. \\ \quad + \int_0^{s_1} \frac{\lambda(\tau)(1-(1-p_{\text{blood}})e^{-\gamma(t-\tau)})}{1+\nu(p_H^r(t-\tau, s_1-\tau)+p_A^r(t-\tau, s_1-\tau))} d\tau \\ \quad + \int_{s_1}^{s_2} \frac{\lambda(\tau)(1-(1-p_{\text{blood}})^2 e^{-\gamma(t-\tau)})}{1+\nu(p_H^r(t-\tau, s_1-\tau, s_2-\tau)+p_A^r(t-\tau, s_1-\tau, s_2-\tau))} d\tau \\ \quad \left. + \dots + \int_{s_{N-1}}^{s_{N_{\text{MDA}}}} \frac{\lambda(\tau)(1-(1-p_{\text{blood}})^{N_{\text{MDA}}} e^{-\gamma(t-\tau)})}{1+\nu(p_H^r(t-\tau, s_1-\tau, \dots, s_{N_{\text{MDA}}}-\tau)+p_A^r(t-\tau, s_1-\tau, \dots, s_{N_{\text{MDA}}}-\tau))} d\tau\right\} & \text{if } t \geq s_{N_{\text{MDA}}}. \end{cases} \tag{S15}
\end{aligned}$$

### S1.3 Probability liver-stage infected individual has one hypnozoite in liver: $k_1(t)$

The probability that a liver-stage infected individual has one hypnozoite in the liver at time  $t$  (that is, the conditional probability for  $N_H(t)$  given an individual does not have an ongoing blood-stage infection at time  $t$ ) under  $N$  MDA rounds is

$$\begin{aligned}
k_1(t) & = P(N_H(t) = 1 | N_A(t) = N_P(t) = 0, N_H(t) > 0), \\
& = \frac{P(N_H(t) = 1 | N_A(t) = N_P(t) = 0)}{1 - P(N_H(t) = 0 | N_A(t) = N_P(t) = 0)}, \\
& = \frac{\exp\{g(0, t) - g(1, t)\}}{1 - P(N_H(t) = 0 | N_A(t) = N_P(t) = 0)} \frac{\partial g(0, t)}{\partial z}, \\
& = \frac{P(N_H(t) = N_A(t) = N_P(t) = 0)}{(1 - P(N_H(t) = 0 | N_A(t) = N_P(t) = 0))P(N_A(t) = N_P(t) = 0)} \frac{\partial g(0, t)}{\partial z}, \tag{S16}
\end{aligned}$$

where

$$\begin{aligned}
\frac{\partial g(0, t)}{\partial z} & = \begin{cases} \int_0^t \frac{\lambda(\tau)\nu p_H(t-\tau)(1-e^{-\gamma(t-\tau)})}{[1+\nu(p_H(t-\tau)+p_A(t-\tau))]^2} d\tau & \text{if } t < s_1, \\ \int_{s_1}^t \frac{\lambda(\tau)\nu p_H(t-\tau)(1-e^{-\gamma(t-\tau)})}{[1+\nu(p_H(t-\tau)+p_A(t-\tau))]^2} d\tau \\ \quad + \int_0^{s_1} \frac{\lambda(\tau)\nu p_H^r(t-\tau, s_1-\tau)(1-(1-p_{\text{blood}})e^{-\gamma(t-\tau)})}{[1+\nu(p_H^r(t-\tau, s_1-\tau)+p_A^r(t-\tau, s_1-\tau))]^2} d\tau \\ \quad + \int_{s_1}^{s_2} \frac{\lambda(\tau)\nu p_H^r(t-\tau, s_1-\tau, s_2-\tau)(1-(1-p_{\text{blood}})^2 e^{-\gamma(t-\tau)})}{[1+\nu(p_H^r(t-\tau, s_1-\tau, s_2-\tau)+p_A^r(t-\tau, s_1-\tau, s_2-\tau))]^2} d\tau & \text{if } s_1 \leq t < s_2, \\ \vdots \\ \int_{s_{N_{\text{MDA}}}}^t \frac{\lambda(\tau)\nu p_H(t-\tau)(1-e^{-\gamma(t-\tau)})}{[1+\nu(p_H(t-\tau)+p_A(t-\tau))]^2} d\tau \\ \quad + \int_0^{s_1} \frac{\lambda(\tau)\nu p_H^r(t-\tau, s_1-\tau)(1-(1-p_{\text{blood}})e^{-\gamma(t-\tau)})}{[1+\nu(p_H^r(t-\tau, s_1-\tau)+p_A^r(t-\tau, s_1-\tau))]^2} d\tau \\ \quad + \int_{s_1}^{s_2} \frac{\lambda(\tau)\nu p_H^r(t-\tau, s_1-\tau, s_2-\tau)(1-(1-p_{\text{blood}})^2 e^{-\gamma(t-\tau)})}{[1+\nu(p_H^r(t-\tau, s_1-\tau, s_2-\tau)+p_A^r(t-\tau, s_1-\tau, s_2-\tau))]^2} d\tau \\ \quad \left. + \dots + \int_{s_{N-1}}^{s_{N_{\text{MDA}}}} \frac{\lambda(\tau)\nu p_H^r(t-\tau, s_1-\tau, \dots, s_{N_{\text{MDA}}}-\tau)(1-(1-p_{\text{blood}})^{N_{\text{MDA}}} e^{-\gamma(t-\tau)})}{[1+\nu(p_H^r(t-\tau, s_1-\tau, \dots, s_{N_{\text{MDA}}}-\tau)+p_A^r(t-\tau, s_1-\tau, \dots, s_{N_{\text{MDA}}}-\tau))]^2} d\tau \right. & \text{if } t \geq s_{N_{\text{MDA}}}. \end{cases} \tag{S17}
\end{aligned}$$

Here, the expression

$$P(N_H(t) = 1 | N_A(t) = N_P(t) = 0) = \exp \{g(0, t) - g(1, t)\} \frac{\partial g(0, t)}{\partial z}$$

follows from Equation (78) in Mehra *et al.* [24] and  $P(N_H(t) = 0 | N_A(t) = N_P(t) = 0)$  is obtained by dividing Equation (S15) by Equation (S14).

## S1.4 Average number of hypnozoites within liver-stage infected individuals: $k_T(t)$

The average number of hypnozoites within liver-stage infected individuals,  $k_T(t)$ , is defined in Anwar *et al.* 2023 [18] as

$$k_T = \sum_{i=1}^{\infty} i k_i = \left( \frac{\mathbb{E} [N_H(t) | N_A(t) = N_P(t) = 0]}{1 - P(N_H(t) = 0 | N_A(t) = N_P(t) = 0)} \right),$$

where  $\mathbb{E} [N_H(t) | N_A(t) = N_P(t) = 0]$  is the expected size of the hypnozoite reservoir in an uninfected (no blood-stage infection) individual under  $N$  rounds of MDA and is given by

$$\begin{aligned} & \mathbb{E} [N_H(t) | N_A(t) = N_P(t) = 0] \\ &= \begin{cases} \int_0^t \frac{\nu p_H(t-\tau) \lambda(\tau) (1 - e^{-\gamma(t-\tau)})}{[1 + \nu p_A(t-\tau)]^2} d\tau & \text{if } t < s_1, \\ \int_{s_1}^t \frac{\nu p_H(t-\tau) \lambda(\tau) (1 - e^{-\gamma(t-\tau)})}{[1 + \nu p_A(t-\tau)]^2} d\tau \\ \quad + \int_0^{s_1} \frac{\nu p_H^r(t-\tau, s_1-\tau) \lambda(\tau) (1 - (1 - p_{\text{blood}}) e^{-\gamma(t-\tau)})}{[1 + \nu p_A^r(t-\tau, s_1-\tau)]^2} d\tau \\ \quad + \int_{s_1}^{s_2} \frac{\nu p_H^r(t-\tau, s_1-\tau, s_2-\tau) \lambda(\tau) (1 - (1 - p_{\text{blood}})^2 e^{-\gamma(t-\tau)})}{[1 + \nu p_A^r(t-\tau, s_1-\tau, s_2-\tau)]^2} d\tau & \text{if } s_1 \leq t < s_2, \\ \vdots \\ \int_{s_{N_{\text{MDA}}}}^t \frac{\nu p_H(t-\tau) \lambda(\tau) (1 - e^{-\gamma(t-\tau)})}{[1 + \nu p_A(t-\tau)]^2} d\tau \\ \quad + \int_0^{s_1} \frac{\nu p_H^r(t-\tau, s_1-\tau) \lambda(\tau) (1 - (1 - p_{\text{blood}}) e^{-\gamma(t-\tau)})}{[1 + \nu p_A^r(t-\tau, s_1-\tau)]^2} d\tau \\ \quad + \int_{s_1}^{s_2} \frac{\nu p_H^r(t-\tau, s_1-\tau, s_2-\tau) \lambda(\tau) (1 - (1 - p_{\text{blood}})^2 e^{-\gamma(t-\tau)})}{[1 + \nu p_A^r(t-\tau, s_1-\tau, s_2-\tau)]^2} d\tau \\ \quad + \dots + \int_{s_{N-1}}^{s_{N_{\text{MDA}}}} \frac{\nu p_H^r(t-\tau, s_1-\tau, \dots, s_{N_{\text{MDA}}}-\tau) \lambda(\tau) (1 - (1 - p_{\text{blood}})^{N_{\text{MDA}}} e^{-\gamma(t-\tau)})}{[1 + \nu p_A^r(t-\tau, s_1-\tau, \dots, s_{N_{\text{MDA}}}-\tau)]^2} d\tau & \text{if } t \geq s_{N_{\text{MDA}}}. \end{cases} \end{aligned} \tag{S18}$$

## S2 Recovery with superinfection

When considering superinfection, an individual experiences multiple (at least one) blood-stage infections (either from a new infectious bite or hypnozoite activation) at the same time. We define the multiplicity of infection (*MOI*) as the number of distinct parasite broods co-circulating within a blood-stage infected individual from different infections. Thus, *MOI* is given by the total number of blood-stage infections (infections from mosquito bites and relapses) at time  $t$ :  $M_I(t) = N_A(t) + N_P(t)$ , where  $N_A$  and  $N_P$  represent the number of relapse and primary infections at time  $t$ . Thus, the probability of recovery from a blood-stage infection ( $I$ ) is conditional upon how many infections

(*MOI*) they are currently experiencing. As per Mehra *et al.* [54] and Näsell *et al.* [55], the recovery rate under superinfection is

$$\begin{aligned} \text{Recovery rate} &= \gamma P(N_A(t) + N_P(t) = 1 | P(N_A(t) + N_P(t) > 0), \\ &= \frac{\gamma P(N_A(t) + N_P(t) = 1)}{P(N_A(t) + N_P(t) > 0)}, \end{aligned} \quad (\text{S19})$$

where  $\gamma$  is the recovery rate without superinfection. The recovery rate is conditioned upon having at least one infection at a time  $t$ , and after the recovery, individuals move out of the blood-stage infected compartment ( $I$ ). Previously, in our model without superinfection (Anwar *et al.* 2022 [17]), individuals from the blood-stage infected compartment ( $I$ ) compartment move to the susceptible compartment ( $S$ ) at rate  $\gamma p(t)$  and move to the liver-stage infected compartment ( $L$ ) at rate  $\gamma(1 - p(t))$  because of the assumption of a constant recovery rate,  $\gamma$ . That is, we only needed the hypnozoite distribution given an individual in the blood-stage infected compartment. However, with superinfection, individuals from the blood-stage infected compartment ( $I$ ) will move back to the susceptible compartment ( $S$ ) if they are experiencing only one infection and have no hypnozoites. That is, the recovery rate depends upon the multiplicity of infection and hypnozoite status, which means the probability  $p(t)$  is insufficient to characterise the dynamics. Therefore, we need the joint probability of experiencing only one infection together with the hypnozoite reservoir size.

## S2.1 Probability of blood-stage infected individual having one infection and no hypnozoites: $p_1(t)$

Following the work of Mehra [54], we define  $p_1(t)$  to be the probability that a blood-stage infected individual has no hypnozoites and is experiencing only one infection at time  $t$ . That is,

$$\begin{aligned} p_1(t) &= P(N_A(t) + N_P(t) = 1, N_H(t) = 0 | P(N_A(t) + N_P(t) > 0), \\ &= \frac{P(N_A(t) + N_P(t) = 1, N_H(t) = 0)}{P(N_A(t) + N_P(t) > 0)}, \\ &= \frac{P(N_A(t) + N_P(t) = 1 | N_H(t) = 0) P(N_H(t) = 0)}{1 - P(N_A(t) + N_P(t) = 0)}, \end{aligned} \quad (\text{S20})$$

where the expression for  $P(N_H(t) = 0)$  and  $P(N_A(t) + N_P(t) = 0)$  follows from Equations (S13) and (S14).

Now, multiplicity of infection given an empty hypnozoite reservoir,  $P(N_A(t) + N_P(t) | N_H(t) = 0)$ , can be obtained from the PGF given by Equation (S10) that holds for before treatment and by Equation (S11) which holds following treatment at times  $t = s_1, s_2, \dots, s_{N_{\text{MDA}}}$  as

$$\begin{aligned} \mathbb{E}[z^{M_I(t)} | N_H(t) = 0] &= \begin{cases} \frac{G(t, z_H=0, z_A=z, z_C=1, z_D=1, z_P=z z_{PC}=1)}{G(t, z_H=0, z_A=1, z_C=1, z_D=1, z_P=1 z_{PC}=1)} & \text{if } t < s_1 \\ \frac{G^{s_1}(t, z_H=0, z_A=z, z_C=1, z_D=1, z_P=z z_{PC}=1)}{G^{s_1}(t, z_H=0, z_A=1, z_C=1, z_D=1, z_P=1 z_{PC}=1)} & \text{if } s_1 \leq t < s_2, \\ \vdots & \\ \frac{G^{s_1, s_2, \dots, s_{N_{\text{MDA}}}}(t, z_H=0, z_A=z, z_C=1, z_D=1, z_P=z z_{PC}=1)}{G^{s_1, s_2, \dots, s_{N_{\text{MDA}}}}(t, z_H=0, z_A=1, z_C=1, z_D=1, z_P=1 z_{PC}=1)} & \text{if } t \geq s_{N_{\text{MDA}}}, \end{cases} \\ &= \exp\{h(z, t) - h(1, t)\}, \end{aligned}$$

where

$$h(z, t) = \begin{cases} \int_0^t \lambda(\tau) \frac{ze^{-\gamma(t-\tau)} + (1-e^{-\gamma(t-\tau)})}{1 + (p_H(t-\tau) + (1-z)p_A(t-\tau))^\nu} d\tau & \text{if } t < s_1 \\ \int_{s_1}^t \lambda(\tau) \frac{ze^{-\gamma(t-\tau)} + (1-e^{-\gamma(t-\tau)})}{1 + (p_H(t-\tau) + (1-z)p_A(t-\tau))^\nu} d\tau \\ + \int_0^{s_1} \lambda(\tau) \frac{z(1-p_{blood})e^{-\gamma(t-\tau)} + (1-(1-p_{blood})e^{-\gamma(t-\tau)})}{1 + (p_H(t-\tau, s_1-\tau) + (1-z)p_A(t-\tau, s_1-\tau))^\nu} d\tau & \text{if } s_1 \leq t < s_2, \\ \vdots \\ \int_{s_{N_{MDA}}}^t \lambda(\tau) \frac{ze^{-\gamma(t-\tau)} + (1-e^{-\gamma(t-\tau)})}{1 + (p_H(t-\tau) + (1-z)p_A(t-\tau))^\nu} d\tau \\ + \int_0^{s_1} \lambda(\tau) \frac{z(1-p_{blood})e^{-\gamma(t-\tau)} + (1-(1-p_{blood})e^{-\gamma(t-\tau)})}{1 + (p_H(t-\tau, s_1-\tau) + (1-z)p_A(t-\tau, s_1-\tau))^\nu} d\tau \\ + \dots + \int_{s_{N-1}}^{s_{N_{MDA}}} \lambda(\tau) \frac{z(1-p_{blood})^{N_{MDA}}e^{-\gamma(t-\tau)} + (1-(1-p_{blood})^{N_{MDA}}e^{-\gamma(t-\tau)})}{1 + (p_H(t-\tau, s_1-\tau, \dots, s_{N_{MDA}}-\tau) + (1-z)p_A(t-\tau, s_1-\tau, \dots, s_{N_{MDA}}-\tau))^\nu} d\tau & \text{if } t \geq s_{N_{MDA}}. \end{cases} \quad (S21)$$

Now, the PMF for  $M_I(t)|N_H(t) = 0$  is

$$\begin{aligned} P(N_A(t) + N_P(t) = n | N_H(t) = 0) &= P(M_I(t) = n | N_H(t) = 0), \\ &= \exp \{h(0, t) - h(1, t)\} \frac{1}{n!} \sum_{k=1}^n B_{n,k} \left[ \frac{\partial h(0, t)}{\partial z}, \frac{\partial^2 h(0, t)}{\partial z^2}, \dots, \frac{\partial^{n-k+1} h(0, t)}{\partial z^{n-k+1}} \right], \end{aligned}$$

where

$$\frac{\partial^k h}{\partial z^k}(0, t) = \begin{cases} k! \int_0^t \frac{\lambda(\tau) [\nu p_A(t-\tau)]^{k-1}}{[1 + \nu(p_A(t-\tau) + p_H(t-\tau))]^k} \left( e^{-\gamma(t-\tau)} + \frac{\nu p_A(t-\tau)(1-e^{-\gamma(t-\tau)})}{1 + \nu p_A(t-\tau)} \right) d\tau & \text{if } t < s_1 \\ k! \left( \int_{s_1}^t \frac{\lambda(\tau) \nu p_A(t-\tau)^{k-1}}{[1 + \nu(p_A(t-\tau) + p_H(t-\tau))]^k} \left( e^{-\gamma(t-\tau)} + \frac{\nu p_A(t-\tau)(1-e^{-\gamma(t-\tau)})}{1 + \nu p_A(t-\tau)} \right) d\tau \right. \\ + \int_0^{s_1} \frac{\lambda(\tau) \nu p_A^r(t-\tau, s_1-\tau)^{k-1}}{[1 + \nu(p_A^r(t-\tau, s_1-\tau) + p_H^r(t-\tau, s_1-\tau))]^k} \left( (1-p_{blood})e^{-\gamma(t-\tau)} \right. \\ \left. + \frac{\nu p_A^r(t-\tau, s_1-\tau)(1-(1-p_{blood})e^{-\gamma(t-\tau)})}{1 + \nu p_A^r(t-\tau, s_1-\tau)} \right) d\tau & \text{if } s_1 \leq t < s_2, \\ \vdots \\ k! \left( \int_{s_{N_{MDA}}}^t \frac{\lambda(\tau) \nu p_A(t-\tau)^{k-1}}{[1 + \nu(p_A(t-\tau) + p_H(t-\tau))]^k} \left( e^{-\gamma(t-\tau)} + \frac{\nu p_A(t-\tau)(1-e^{-\gamma(t-\tau)})}{1 + \nu p_A(t-\tau)} \right) d\tau \right. \\ + \int_0^{s_1} \frac{\lambda(\tau) \nu p_A^r(t-\tau, s_1-\tau)^{k-1}}{[1 + \nu(p_A^r(t-\tau, s_1-\tau) + p_H^r(t-\tau, s_1-\tau))]^k} \left( (1-p_{blood})e^{-\gamma(t-\tau)} \right. \\ \left. + \frac{\nu p_A^r(t-\tau, s_1-\tau)(1-(1-p_{blood})e^{-\gamma(t-\tau)})}{1 + \nu p_A^r(t-\tau, s_1-\tau)} \right) d\tau + \dots \\ + \int_{s_{N-1}}^{s_{N_{MDA}}} \frac{\lambda(\tau) \nu p_A^r(t-\tau, s_1-\tau, \dots, s_{N_{MDA}}-\tau)^{k-1}}{[1 + \nu(p_A^r(t-\tau, s_1-\tau, \dots, s_{N_{MDA}}-\tau) + p_H^r(t-\tau, s_1-\tau, \dots, s_{N_{MDA}}-\tau))]^k} \\ \left. \left( (1-p_{blood})^N e^{-\gamma(t-\tau)} + \frac{\nu p_A^r(t-\tau, s_1-\tau, \dots, s_{N_{MDA}}-\tau)(1-(1-p_{blood})^N e^{-\gamma(t-\tau)})}{1 + \nu p_A^r(t-\tau, s_1-\tau, \dots, s_{N_{MDA}}-\tau)} \right) d\tau \right) & \text{if } t \geq s_{N_{MDA}}. \end{cases}$$

Therefore,

$$\begin{aligned}
P(N_A(t) + N_P(t) = 1 | N_H(t) = 0) &= \exp \{h(0, t) - h(1, t)\} \frac{\partial h(0, t)}{\partial z}, \\
&= \frac{G(t, z_H = 0, z_A = 0, z_C = 1, z_D = 1, z_P = 0, z_{PC} = 1)}{G(t, z_H = 0, z_A = 1, z_C = 1, z_D = 1, z_P = 1, z_{PC} = 1)} \frac{\partial h(0, t)}{\partial z}, \\
&= \frac{P(N_H(t) = N_A(t) = N_P(t) = 0)}{P(N_H(t) = 0)} \frac{\partial h(0, t)}{\partial z}.
\end{aligned}$$

Finally, from Equation (S20)

$$\begin{aligned}
p_1(t) &= \frac{P(N_A(t) + N_P(t) = 1 | N_H(t) = 0) P(N_H(t) = 0)}{1 - P(N_A(t) + N_P(t) = 0)}, \\
&= \frac{P(N_H(t) = N_A(t) = N_P(t) = 0)}{1 - P(N_A(t) = N_P(t) = 0)} \frac{\partial h(0, t)}{\partial z},
\end{aligned} \tag{S22}$$

where

$$\frac{\partial h(0, t)}{\partial z} = \begin{cases} \int_0^t \lambda(\tau) \frac{e^{-\gamma(t-\tau)} (1 + \nu p_H(t-\tau) + \nu p_A(t-\tau))}{[1 + \nu (p_A(t-\tau) + p_H(t-\tau))]^2} d\tau & \text{if } t < s_1, \\ \int_{s_1}^t \lambda(\tau) \frac{e^{-\gamma(t-\tau)} (1 + \nu p_H(t-\tau) + \nu p_A(t-\tau))}{[1 + \nu (p_A(t-\tau) + p_H(t-\tau))]^2} d\tau \\ + \int_0^{s_1} \lambda(\tau) \frac{(1 - p_{\text{blood}}) e^{-\gamma(t-\tau)} (1 + \nu p_H^r(t-\tau, s_1 - \tau) + \nu p_A^r(t-\tau, s_1 - \tau))}{[1 + \nu (p_A^r(t-\tau, s_1 - \tau) + p_H^r(t-\tau, s_1 - \tau))]^2} d\tau \\ + \int_{s_1}^{s_2} \lambda(\tau) \frac{(1 - p_{\text{blood}})^2 e^{-\gamma(t-\tau)} (1 + \nu p_H^r(t-\tau, s_1 - \tau, s_2 - \tau) + \nu p_A^r(t-\tau, s_1 - \tau, s_2 - \tau))}{[1 + \nu (p_A^r(t-\tau, s_1 - \tau, s_{N_{\text{MDA}}}) - \tau) + p_H^r(t-\tau, s_1 - \tau, s_{N_{\text{MDA}}}) - \tau)]^2} d\tau & \text{if } s_1 \leq t < s_2, \\ \vdots \\ \int_{s_{N_{\text{MDA}}}}^t \lambda(\tau) \frac{e^{-\gamma(t-\tau)} (1 + \nu p_H(t-\tau) + \nu p_A(t-\tau))}{[1 + \nu (p_A(t-\tau) + p_H(t-\tau))]^2} d\tau \\ + \int_0^{s_1} \lambda(\tau) \frac{(1 - p_{\text{blood}}) e^{-\gamma(t-\tau)} (1 + \nu p_H^r(t-\tau, s_1 - \tau) + \nu p_A^r(t-\tau, s_1 - \tau))}{[1 + \nu (p_A^r(t-\tau, s_1 - \tau) + p_H^r(t-\tau, s_1 - \tau))]^2} d\tau \\ + \int_{s_1}^{s_2} \lambda(\tau) \frac{(1 - p_{\text{blood}})^2 e^{-\gamma(t-\tau)} (1 + \nu p_H^r(t-\tau, s_1 - \tau, s_2 - \tau) + \nu p_A^r(t-\tau, s_1 - \tau, s_2 - \tau))}{[1 + \nu (p_A^r(t-\tau, s_1 - \tau, s_{N_{\text{MDA}}}) - \tau) + p_H^r(t-\tau, s_1 - \tau, s_{N_{\text{MDA}}}) - \tau)]^2} d\tau \\ + \dots + \int_{s_{N-1}}^{s_{N_{\text{MDA}}}} \lambda(\tau) \left[ \frac{(1 - p_{\text{blood}})^{N_{\text{MDA}}} e^{-\gamma(t-\tau)} (1 + \nu p_H^r(t-\tau, s_1 - \tau, \dots, s_{N_{\text{MDA}}}) - \tau)}{[1 + \nu (p_A^r(t-\tau, s_1 - \tau, \dots, s_{N_{\text{MDA}}}) - \tau) + p_H^r(t-\tau, s_1 - \tau, \dots, s_{N_{\text{MDA}}}) - \tau)]^2} \right. \\ \left. + \frac{\nu p_A^r(t-\tau, s_1 - \tau, \dots, s_{N_{\text{MDA}}}) - \tau}{[1 + \nu (p_A^r(t-\tau, s_1 - \tau, \dots, s_{N_{\text{MDA}}}) - \tau) + p_H^r(t-\tau, s_1 - \tau, \dots, s_{N_{\text{MDA}}}) - \tau)]^2} \right] d\tau & \text{if } t \geq s_{N_{\text{MDA}}}. \end{cases}$$

## S2.2 Probability of blood-stage infected individual having one infection and non-zero hypnozoites: $p_2(t)$

Meanwhile, individuals in  $I$  move to  $L$  after recovery if they have hypnozoites. We define  $p_2(t)$  to be the probability that a blood-stage infected individual has hypnozoites and is experiencing



more than one blood-stage infection at time  $t$ . That is,

$$\begin{aligned}
p_2(t) &= P(N_A(t) + N_P(t) = 1, N_H(t) > 0 | P(N_A(t) + N_P(t) > 0), \\
&= \frac{P(N_A(t) + N_P(t) = 1, N_H(t) > 0)}{P(N_A(t) + N_P(t) > 0)}, \\
&= \frac{P(N_A(t) + N_P(t) = 1 | N_H(t) > 0) P(N_H(t) > 0)}{1 - P(N_A(t) + N_P(t) = 0)}, \\
&= \frac{P(N_A(t) + N_P(t) = 1) - P(N_A(t) + N_P(t) = 1 | N_H(t) = 0) P(N_H(t) = 0)}{1 - P(N_A(t) + N_P(t) = 0)}, \\
&= \frac{P(N_A(t) + N_P(t) = 1)}{1 - P(N_A(t) + N_P(t) = 0)} - p_1(t). \tag{S23}
\end{aligned}$$

The expression  $P(N_A(t) + N_P(t) = 0) = P(N_A(t) = N_P(t) = 0)$  is given by Equation (S14). The expression for  $P(N_A(t) + N_P(t) = 1)$  follows from Equation (81) in Mehra *et al.* [24] and is given by

$$P(N_A(t) + N_P(t) = 1) = P(N_A(t) = N_P(t) = 0) \frac{\partial f(0, t)}{\partial z},$$

where

$$\frac{\partial f(0, t)}{\partial z} = \begin{cases} \int_0^t \lambda(\tau) \frac{e^{-\gamma(t-\tau)} + \nu p_A(t-\tau)}{[1 + \nu p_A(t-\tau)]^2} d\tau & \text{if } t < s_1, \\ \int_{s_1}^t \lambda(\tau) \frac{e^{-\gamma(t-\tau)} + \nu p_A(t-\tau)}{[1 + \nu p_A(t-\tau)]^2} d\tau \\ + \int_0^{s_1} \lambda(\tau) \frac{(1-p_{\text{blood}})e^{-\gamma(t-\tau)} + \nu p_A^r(t-\tau, s_1-\tau)}{[1 + \nu p_A^r(t-\tau, s_1-\tau)]^2} d\tau \\ + \int_{s_1}^{s_2} \lambda(\tau) \frac{(1-p_{\text{blood}})^2 e^{-\gamma(t-\tau)} + \nu p_A^r(t-\tau, s_1-\tau, s_2-\tau)}{[1 + \nu p_A^r(t-\tau, s_1-\tau, s_2-\tau)]^2} d\tau \\ + \dots + \int_{s_{N-1}}^{s_{N_{\text{MDA}}}} \lambda(\tau) \frac{(1-p_{\text{blood}})^{N_{\text{MDA}}} e^{-\gamma(t-\tau)} + \nu p_A^r(t-\tau, s_1-\tau, \dots, s_{N_{\text{MDA}}}-\tau)}{[1 + \nu p_A^r(t-\tau, s_1-\tau, \dots, s_{N_{\text{MDA}}}-\tau)]^2} d\tau & \text{if } s_1 \leq t < s_2, \\ \vdots \\ \int_{s_{N_{\text{MDA}}}}^t \lambda(\tau) \frac{e^{-\gamma(t-\tau)} + \nu p_A(t-\tau)}{[1 + \nu p_A(t-\tau)]^2} d\tau \\ + \int_0^{s_1} \lambda(\tau) \frac{(1-p_{\text{blood}})e^{-\gamma(t-\tau)} + \nu p_A^r(t-\tau, s_1-\tau)}{[1 + \nu p_A^r(t-\tau, s_1-\tau)]^2} d\tau \\ + \int_{s_1}^{s_2} \lambda(\tau) \frac{(1-p_{\text{blood}})^2 e^{-\gamma(t-\tau)} + \nu p_A^r(t-\tau, s_1-\tau, s_2-\tau)}{[1 + \nu p_A^r(t-\tau, s_1-\tau, s_2-\tau)]^2} d\tau \\ + \dots + \int_{s_{N-1}}^{s_{N_{\text{MDA}}}} \lambda(\tau) \frac{(1-p_{\text{blood}})^{N_{\text{MDA}}} e^{-\gamma(t-\tau)} + \nu p_A^r(t-\tau, s_1-\tau, \dots, s_{N_{\text{MDA}}}-\tau)}{[1 + \nu p_A^r(t-\tau, s_1-\tau, \dots, s_{N_{\text{MDA}}}-\tau)]^2} d\tau & \text{if } t \geq s_{N_{\text{MDA}}}. \end{cases}$$

The time-dependent probabilities  $p(t)$ ,  $p_1(t)$ ,  $p_2(t)$ ,  $k_1(t)$ , and  $k_T(t)$  that characterise the hypnozoite dynamics at the population level, account for all the infective bites received throughout time (as a function of  $\lambda(t)$ ) and change instantaneously with MDA because of the assumption of the instantaneous effect of the drug.

Table S1: Optimal interval for up to four rounds of MDA obtained from the deterministic version of the model.

Prevalence		10%	20%	30%	40%	50%	60%	70%	80%	90%	
Interval (days)	One round	$x_0$ (Peak to MDA1)	116.4	116.4	116.4	102.4	102.4	102.4	69	69	58.7
	Two rounds	$x_0$ (Peak to MDA1)	139.9	139.9	139.9	139.9	139.9	139.9	101.8	101.8	101.8
		$x_1$ (MDA1 to MDA2)	28.6	28.6	28.6	28.6	28.6	28.6	303.4	303.4	303.4
	Three rounds	$x_0$ (Peak to MDA1)	10	139.9	139.9	139.9	139.9	139.9	116.4	116.4	116.4
		$x_1$ (MDA1 to MDA2)	10	28.6	28.6	28.6	28.6	28.6	116.4	116.4	116.4
		$x_2$ (MDA2 to MDA3)	10	53.8	53.8	53.8	53.8	53.8	50.3	50.3	50.3
	Four rounds	$x_0$ (Peak to MDA1)	139.9	139.9	139.9	139.9	139.9	139.9	116.4	116.4	52.7
		$x_1$ (MDA1 to MDA2)	28.6	28.6	28.6	28.6	28.6	28.6	276.6	276.6	325.3
		$x_2$ (MDA2 to MDA3)	53.8	53.8	53.8	53.8	53.8	53.8	50.3	50.3	333.5
		$x_3$ (MDA3 to MDA4)	285	285	285	285	285	285	285	285	88.9

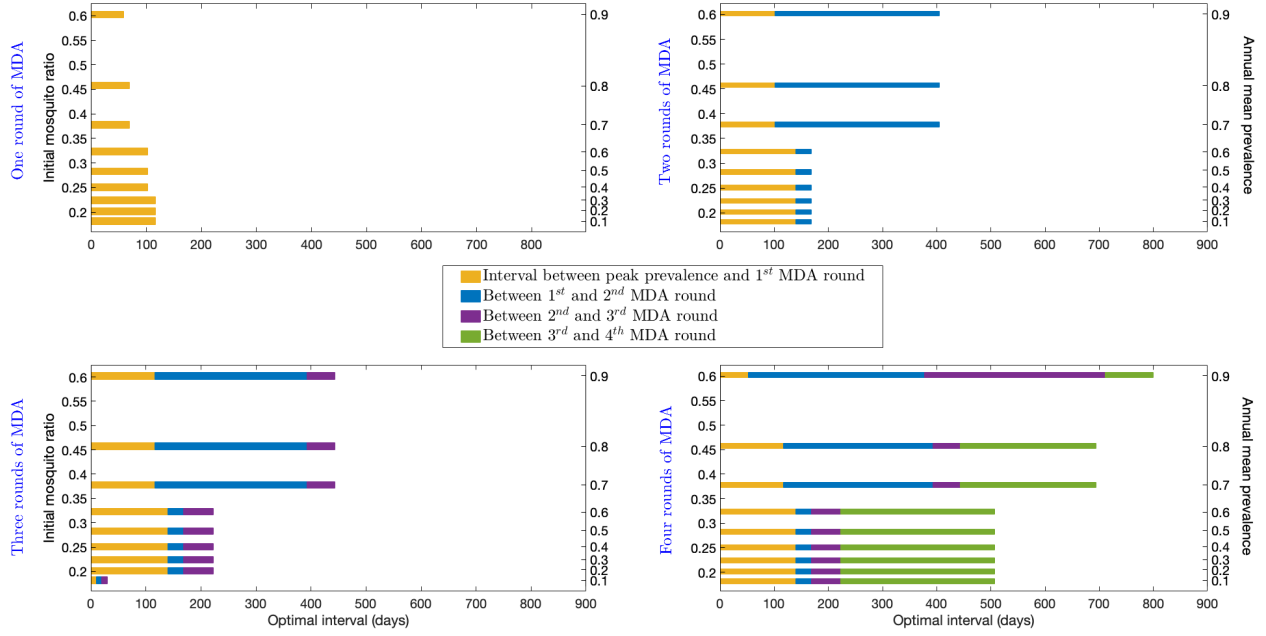


Figure S2: *Optimal MDA intervals for up to four rounds obtained with the deterministic version of the model for varying mosquito to human  $m_0$  (left vertical axis). These different initial mosquito ratios correspond to the prevalence of blood-stage infection in the range of 10–90% (right vertical axis).*